Int J Adv Manuf Technol
DOI 10.1007/s00170-017-0251-z

ORIGINAL ARTICLE

A review on the recent development of incremental sheet-forming process

Yanle Li[1,2] · **Xiaoxiao Chen**[1] · **Zhaobing Liu**[3] · **Jie Sun**[1,2] · **Fangyi Li**[1,2] · **Jianfeng Li**[1,2] · **Guoqun Zhao**[4]

Received: 1 November 2016 / Accepted: 6 March 2017

Abstract This paper presents a detailed literature review on the current research of incremental sheet forming relating to deformation mechanism, modelling techniques, forming force prediction and process investigations. First, a review of the fundamental deformation mechanism and formability in incremental sheet forming (ISF) is provided. Subsequently, the modelling techniques for ISF are reviewed and categorised into two approaches: analytical modelling and finite element modelling. Special interest is given to a critical review regarding the forming forces analysis and prediction during the process. Then, previous publications related to geometric accuracy, surface finish and forming efficiency in ISF are reviewed. Finally, several potential hybrid incremental sheet-forming strategies are discussed. This leads to a statement of conclusion which may act as an inspiration and reference for the researcher.

Keywords Incremental sheet forming · Deformation mechanism · Forming force · Formability · Forming quality

✉ Zhaobing Liu
zhaobingliu@whut.edu.cn; zhaobingliu@hotmail.com

[1] School of Mechanical Engineering, Shandong University, Jinan 250061, China

[2] Key Laboratory of High-efficiency and Clean Mechanical Manufacture at Shandong University, Ministry of Education, Jinan 250061, China

[3] School of Mechanical and Electronic Engineering, Wuhan University of Technology, Wuhan 430070, China

[4] School of Material Science & Engineering, Shandong University, Jinan 250061, China

1 Introduction

Incremental sheet-forming (ISF) technology is an emerging sheet-forming process ideal for rapid prototype and small batch production. In an ISF process, a flat metal sheet is gradually formed into the designed 3D shape using computer numerical control (CNC)-controlled generic forming tool. The process is characterised by the fact that at any time only a small part of the product is actually being formed and that the area of local deformation is moving over the entire product until the desired geometry is obtained. By using this process, useable parts can be formed directly from CAD data with a minimum of specialised tooling. Therefore, ISF is widely accepted as a promising forming process over conventional processes such as deep drawing and stamping [1, 2] for small batch production and custom manufactured products.

ISF was patented in 1967 by Leszak [3] and was proven to be feasible by Kitazawa et al. [4] in forming rotational symmetric parts using aluminium. The capability study of using an ordinary CNC milling machine instead of a special designed machine-tool apparatus was later performed by Jeswiet [5] and Filice [6]. ISF can be interpreted in different ways as shown in Fig. 1. In general, the forming tool follows the pre-designed tool path to deform the material incrementally along a succession of contours until the desired final shape is obtained.

The configuration shown in Fig. 1a belongs to single-point incremental forming (SPIF), in which no particular die is needed. The sheet is deformed by the moving tool which is controlled by numerical codes previously designed and imported to the controller. The second one (Fig. 1b) shows an incremental forming with two tools on both sides of the material. This was also referred to as double-sided incremental forming (DSIF) [7]. Since there is no die needed in these two configurations, it is also called a dieless forming process [1, 8]. The other two configurations (Fig. 1c, d) are classified as two-point incremental

Published online: 03 April 2017

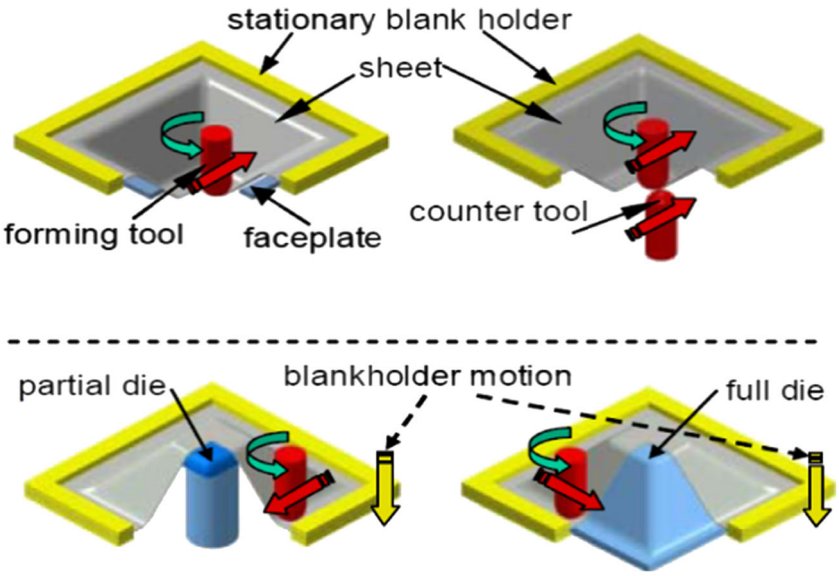

Fig. 1 Four different configurations of ISF process [1]. **a** Single-point incremental forming (SPIF), **b** incremental forming with counter tools, **c** two-point incremental forming (partial die; TPIF), **d** two-point incremental forming (full die; TPIF)

forming (TPIF) where a partial or full die is placed underneath the material. This is commonly used for complex parts to improve the geometric tolerances with no substantial extra cost as dies can be cheaply manufactured with woods or plastics due to low-amplitude forming forces [9].

The ISF process offers the rapid prototyping advantages of short lead times, high flexibility, high formability and lower cost in small batches for aeronautical, automotive and medical applications. Unlike other fast prototyping technologies which are suited to produce dimensionally accurate but non-functional replicas of parts, ISF can be used to produce functional metal parts suitable for use as prototypes, or even as regular production and service parts. ISF has received great attention particularly in the automotive industry.

Figure 2a shows a hood for a Honda S800 model car formed with ISF by Amino Corp. and was finally mounted on an existing vehicle. ISF can also be used for additional forming of an existing production panel for low-volume production. This allows adding features or styles and sharpening the feature lines for the existing manufactured parts. An example is shown in Fig. 2b with logo mark and feature lines formed by ISF. Moreover, ISF is especially favourable to customised products by saving the cost of die fabrication.

The ISF technology has received increasing attention from both academia and industry due to the following advantages:

- Lower forming forces

Since only a small area of the part is being deformed at any time during ISF, the required forming forces are greatly reduced. Therefore, it is possible to use material such as plastics or wood for supporting die. Also, this further enhances the

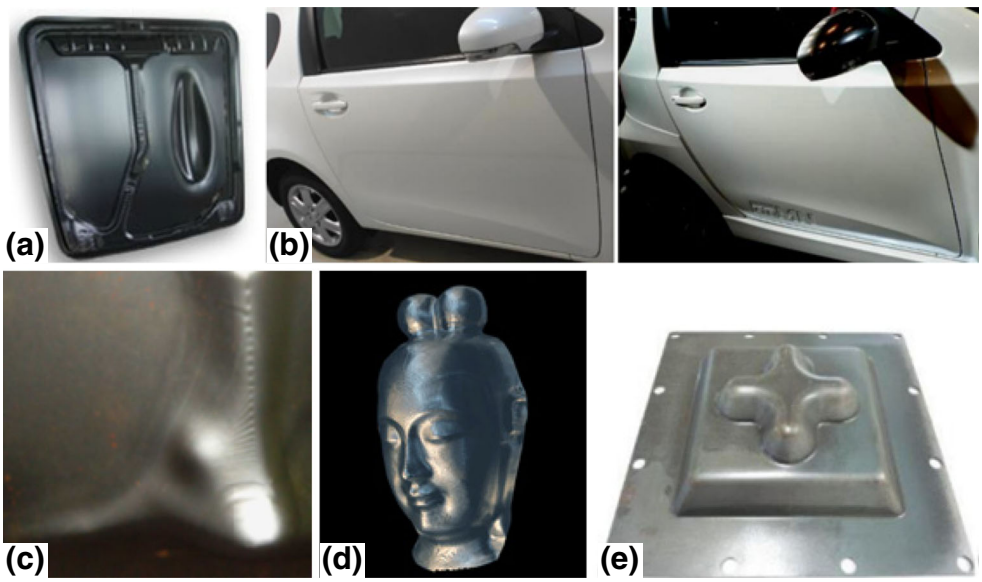

Fig. 2 Applications of ISF: **a** inner side of a hood for Honda S800 model car [8]; **b** normal feature lines of TOYOTA iQ compared with sharpen feature line of TOYOTA iQ-GRMN [8]; **c** customised ankle support [10]; **d** customised Buddha face (AMINO website); **e** sample with 4.5-mm-thickness material of hot rolled steel [8]

forming capacity in terms of both sheet thickness (e.g. 0.1 to 4.0 mm) and also material type (mild steels, aluminium, titanium and even perforated steel mesh).

- Improved formability

Greater formability is achieved in ISF by incrementally deforming the material to the desired shape. As can be seen in Fig. 3a, extensive experimental measurements have shown that the forming limit curve for ISF has a negative slope and is much higher than conventional forming. Figure 3b presents a cone-shaped flower pot formed using ISF technology.

- Lower die tooling cost

Depending on the shape of the part, it may be possible to use a partial die or even eliminate the die in ISF. Figure 4 shows the six different shapes (cone, square, pentagonal, hexagonal, octagonal, dodecagonal) formed by AMINO Corporation [8] using a single blank. The forming die used for these shapes is very simple and only consists of one base plate and six cylindrical posts. The dies can be cheaply made with wood or plastics. Moreover, in ISF, a generic forming tool can manufacture an infinite variety of 3D shapes by adopting careful tool path design. These forming tools are also quite simple with different head shapes as shown in Fig. 5. Comparing with conventional stamping process, the exergy inputs of ISF can be saved more than 64% for producing 50 box parts with AA6022 according to Dittrich et al. [12]. Consequently, the die tooling cost is greatly reduced.

- Flexible forming facilities

Generally, the ISF process can be performed by all CNC-controlled three-axis machines, though large working volumes and sufficient stiffness are favourable. Figure 6 presents some of the commonly used forming machinery for ISF. At the early stage of ISF research, conventional milling machines as shown in Fig. 6a were upgraded by adding a material fixture table. Since 2002, AMINO Corporation started to provide specialised equipment dedicated for ISF to industry globally as shown in Fig. 6b. This equipment features a pneumatic-controlled movable work holder (yellow table in Fig. 6b) which can pre-stretch the material towards the final shape during the forming process. An industrial robot can also be used for the ISF process as shown in Fig. 6c. Some researchers even developed their own ISF machine. Figure 6d shows a prototype fabricated at Northwestern University which focuses on the double-sided incremental forming process. Comparison of facilities with merits and demerits is listed in Table 1.

The above advantages have made ISF a strong potential competitor to conventional sheet-forming processes. However, there are still some limitations in ISF that inhibit extensive industrial applications, as follows:

- Geometric accuracy: This is one of the dominant limits for the further development and commercialisation of the ISF technology. Geometric errors in ISF can be attributed to clamped deviation during forming and unclamped deviation due to residual stresses as well as springback effects.
- Surface finish: This is considered a weak point for ISF products. Surface finish is represented by the large-scale waviness created by the tool path and the small-scale roughness induced by large surface strains. The surface quality is influenced by several process parameters, such as step-down size, tool diameter, sheet thickness, etc.
- Process efficiency: Due to the inherent incremental localised deformation feature, the forming time required to complete the forming process is relatively longer than that of other processes. Nevertheless, the energy consumption which is influenced by both forming time and working load may be attractive by proper process settings.
- Excessive thinning: The final thickness after deformation is an important indicator to evaluate the product quality, especially with larger wall angles (e.g. 70° or more). Excessive thinning narrows the range of geometries that can be produced by ISF.

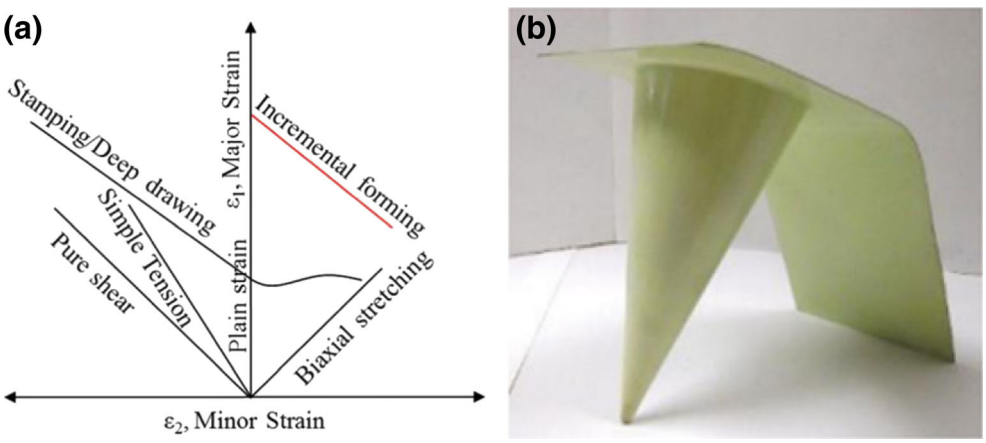

Fig. 3 Improved formability in ISF: **a** forming limit curve for ISF against conventional forming processes [11] and **b** flower pot [8]

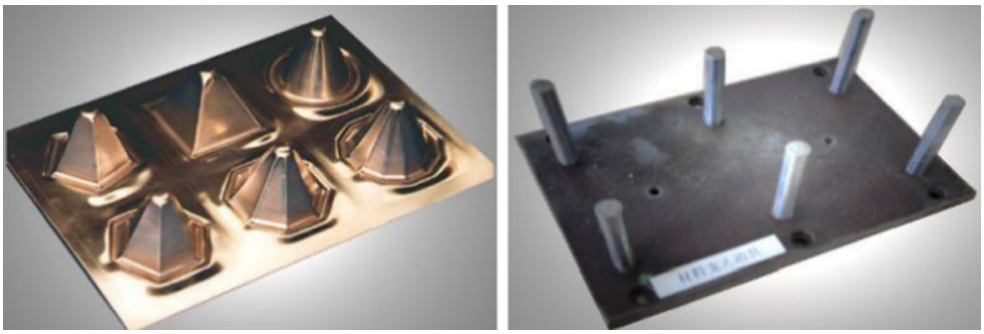

Fig. 4 Variety of pyramid shapes [8]

The above limitations bring some challenges for the further development and commercialisation of ISF, but also motivate the on-going research to promote ISF as a feasible technology on an industrial level.

2 Deformation mechanism and process formability

This section firstly presents a comprehensive review of the current status on the understanding of the deformation mechanism in the ISF process. Then, the strategies to characterise the process formability are reviewed along with the current findings on the effects of process parameters on the ISF process.

2.1 Deformation mechanism

It has been widely acknowledged that ISF has higher formability compared with other conventional forming processes (such as deep drawing and forging) [20, 21] due to its highly localised plastic deformation. The understanding of the fundamental material deformation and fracture mechanism is of great importance for ISF process design and optimisation in achieving enhanced material formability, geometric accuracy and uniform thickness distribution. In recent years, the deformation mechanics behind ISF has been investigated by many researchers through both theoretical analysis [22, 23] and experimental observations [24, 25], but there still remains a lack of a consistent view on how different process parameters affect the deformation behaviour and thus influence the output qualities. This section provides a comprehensive review of the current status on the understanding of the deformation mechanism in the ISF process.

2.1.1 Membrane strain

Several researchers proposed that the dominant deformation mode in ISF process is stretching leading to membrane strain. Silva et al. [22, 23, 26] extensively analysed the single-point incremental forming by means of a membrane approach. A closed-form analytical model was firstly presented which provides insight to the fundamentals behind the fracture of material and the enhanced overall formability of the ISF process. As a result in [22], the membrane analysis of a small plastic zone in rotationally symmetric components was utilised to explain aspects of the formability and damage.

Figure 7 shows the membrane equilibrium conditions of a local shell element analysed by Silva et al. [26]. After neglecting higher-order terms, the simplified forms of these equations can be deduced as follows:

Circumferential direction

$$d\delta_\theta = -\mu_\theta \delta_t \frac{r d_\theta}{t} \approx -\mu_\theta \delta_t \tag{1}$$

Thickness direction

$$\frac{\delta_t}{t} + \frac{\delta_\varnothing}{r_1} + \frac{\delta_\theta}{r_z} = 0 \tag{2}$$

Meridional direction

$$\frac{d\delta_\varnothing}{dr} + \frac{\delta_\varnothing - \delta_\theta}{r} + \frac{\mu_\varnothing \delta_t}{t \sin\alpha} + \frac{\delta_\varnothing}{t}\frac{dt}{dr} = 0 \tag{3}$$

where δ_θ,$\delta_\varnothing$ and δ_t are the circumferential, meridional and thickness stresses, respectively; t is the thickness of the sheet; r is the radial coordinate; r_1 is the radius of curvature of meridian at the element (radius of the SPIF tool) and r_z is the

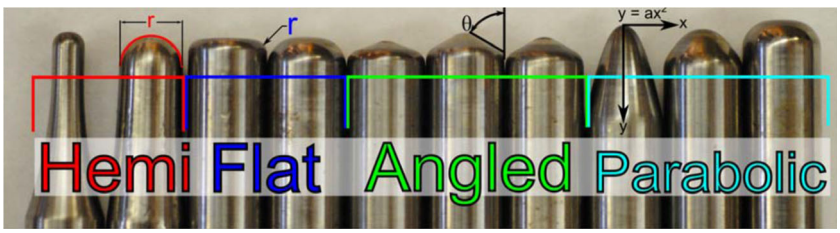

Fig. 5 Variation of forming tool shapes: hemispherical, flat, angled and parabolic [13]

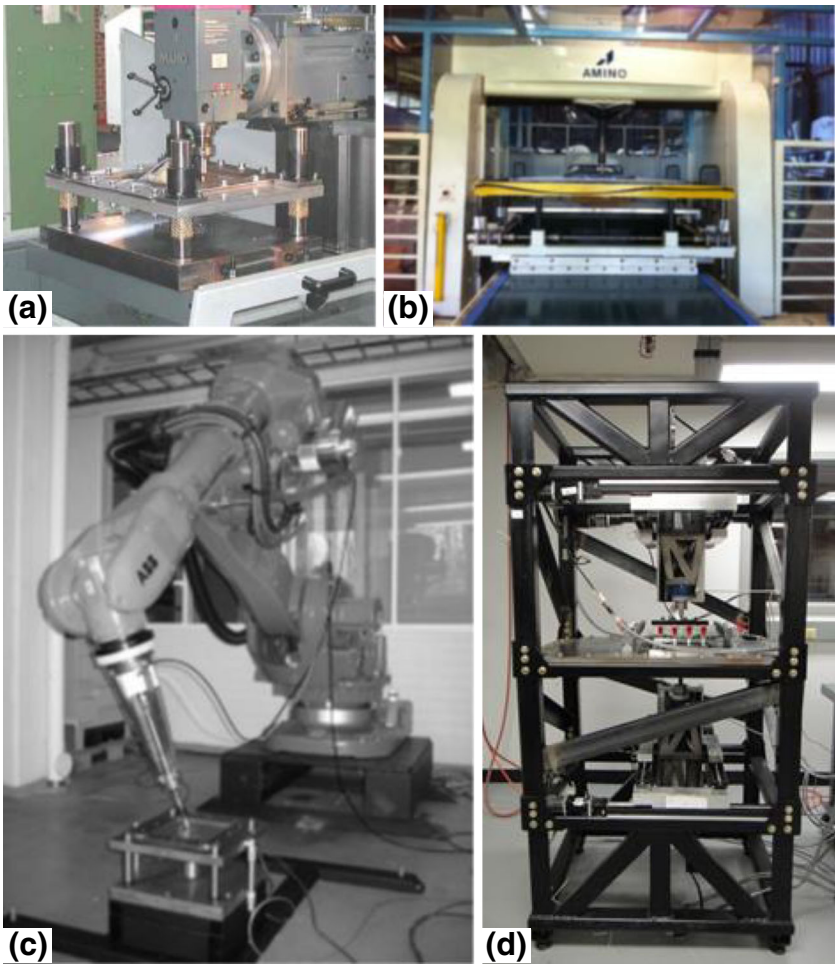

Fig. 6 Forming machinery for ISF: **a** upgraded conventional milling machine for ISF [1]; **b** dedicated AMINO ISF machine [14]; **c** robot-assisted incremental forming [15]; **d** a prototype double-sided incremental forming machine fabricated at Northwestern University [16]

radius of the element normal where it cuts the z-axis.

To simplify the analysis, bending moments of plastically deforming shells were neglected, and the local cells were assumed to be axisymmetric. Meanwhile, the material was assumed to be rigid-perfectly plastic and isotropic.

In this model, all possible tool paths were classified into three basic modes of deformation shown in Fig. 8: (a) flat surfaces under plane strain stretching conditions, (b) rotationally symmetric surfaces under plane strain stretching conditions and (c) corners under equal biaxial stretching conditions. For these three conditions, the states of stress and strain were summarised and compared with those of conventional stamping. According to this analysis, the frictional force exerted at the tool-sheet contact interface can be deduced [26] (see Eqs. (22), (26) and (30)). Further, this model also

Table 1 Comparison of forming facilities with merits and demerits

Types	Researchers	Merits	Demerits
Conventional milling machines	Jeswiet et al. [1]	• Universal • Economical • Easy to adopt	• Size limit • Only for single-point ISF
Self-developed ISF facility	Allwood et al. [17] Cao et al. [16]	• Customised capability • Economical • Suitable for further development	• Non-universal • Limited accuracy • Time-consuming • Size limit
Industrial robot	Vihtonen et al. [15] Duflou et al. [18]	• Flexible set-up • Easy for tool path control	• Stiffness limit • Speed limit
Amino ISF machine	Amino et al. [8] Li et al. [19]	• Enables two-point ISF • Large forming size • Stable and precise	• Non-universal • Expensive

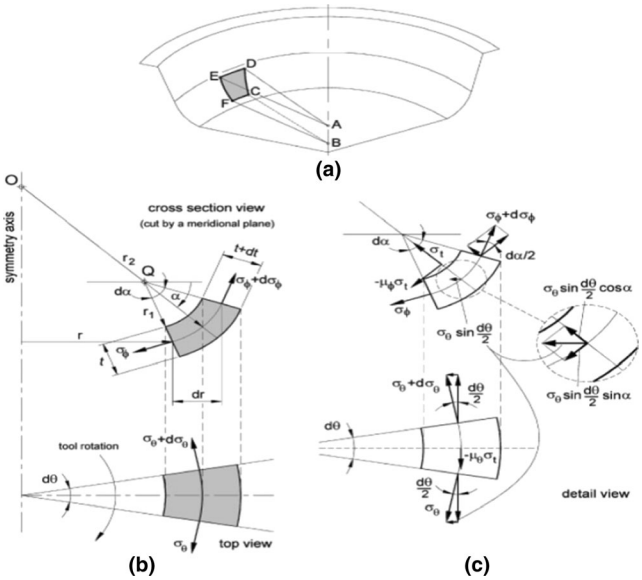

Fig. 7 Rotational symmetric single-point incremental forming: **a** schematic representation of the shell element in perspective; **b** top view of the shell element after being cut by an axial meridional plane; **c** detail of the acting stresses [22]

investigated the sheet thinning at the corner radius and the maximum drawing angle which characterised formability of the process.

2.1.2 Shear deformation

Experimental evidences suggest that the through-thickness shear does exist in ISF and might be one of the main causes for the increased forming limit. Allwood et al. [27] presented the existence of through-thickness shear by modelling a novel simplified process named 'paddle forming' using the commercial finite element software ABAQUS Explicit. This simplified model allows for characterising the trough-thickness shear in a feasible time. It was concluded that the significant shear parallel to the tool motion occurs and this may explain the improved forming limits of the process. Jackson and Allwood [24] further experimentally investigated the strain distributions through the thickness along the cross-sectional plane of the specially prepared copper sheets for both SPIF and TPIF configurations. It was claimed that the deformation mechanism for both cases is stretching and shear in the plane perpendicular to the tool direction together with shear in the plane parallel to the tool direction.

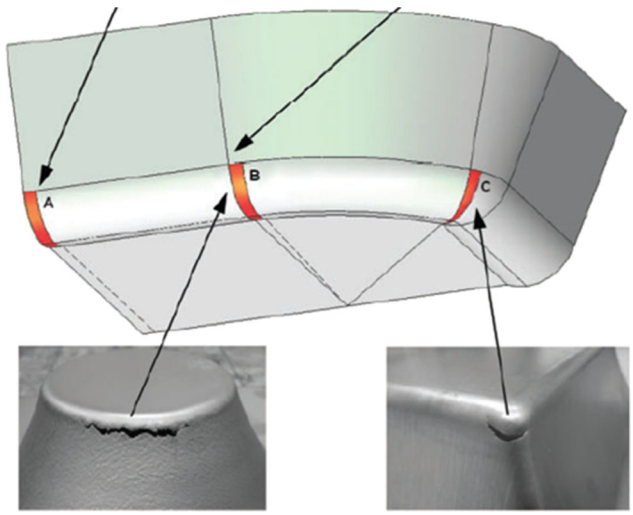

Fig. 8 Instantaneous deformation zone and contact area between forming tool and workpiece during SPIF [26]

Mirnia and Dariani [28] analysed the deformation behaviour of a cone-forming process based on the shear deformation assumption using the upper-bound approach. A series of streamlines defined by the Bezier curves along the forming direction were introduced to represent the deformation zone with no flow in the radial direction. This approach was shown to be effective for predicting the tangential forming force and equivalent strain when the deformation at each step is relatively small. However, the errors between measured and predicted tangential forces become considerably high when the step down is large (e.g. $\Delta z > 0.5$ mm). This trend suggests that the deformation mechanism is related to the forming process parameters, and thus other deformation modes need to be further considered.

Malhotra et al. [29] attempted to predict the occurrence of fracture in SPIF of both a cone and a funnel shape by combining a damage plasticity model proposed by Xue [30] with finite element analyses. They claimed that the fracture of the material is affected mostly by the through-thickness shear and local bending around the forming tool. Lu et al. [31, 32] further discussed the role of friction and through-thickness shear analytically from the stress state point of view and found that the effect of the through-thickness shear caused by the friction is two-sided. The higher shear stress not only potentially enhances the deformation stability, but also increases the stress triaxiality and reduces the formability at the same time.

Eyckens et al. [33] measured the strain distribution during the deformation process using a stereovision system. It was suggested that the dominant deformation mechanism depends on the selected forming parameters (e.g. wall angle and step-down size). They also studied the strain behaviour through a FE model. It was found that a good qualitative agreement has been obtained for the surface strain but the through-thickness shear was not fully captured. Recently, Smith et al. [34] analysed the deformation mechanics of both single-point and accumulative double-sided incremental forming (ADSIF) processes by FE simulation using LS-DYNA explicit software. The authors concluded that the ADSIF could present greater plastic strains, through-thickness shear strains and greater hydrostatic pressure than in SPIF and suggested this might be one of the reasons for the increased formability in ADSIF.

2.1.3 Bending under tension

Emmens and Boogaard [35] performed tensile with bending tests to examine if the bending under tension (BUT) can create large uniform strains. The experimental results proved that a low amount of bending is sufficient to allow large uniform strains of the material. However, it was noticed that a too high bending speed will result in a high pulling force leading to a rapid reduction of the maximum elongation. They [36] also summarised that bending under tensile load plays a critical role in the localised deformation of the ISF process. The mechanism of the BUT is based on the fact that the moving tool causes the sheet to be bent and unbent continuously, so it is only validated when the sheet is being bent. The tensile force is resulted from both the stretching strain and the bending strain. However, since the bending under tension is a dynamic phenomenon with the moving of the tool, more advanced experimental approaches need to be implemented for providing further investigation.

Fang et al. [37] provided a detailed deformation analysis of SPIF with the consideration of both the bending effect and strain hardening. Several sub-zones were divided from the localised deformation region and the state of stress and strain was investigated through the thickness direction. The proposed analytical model was confirmed by both FE simulation and experimental measurements and the model was shown to explain the enhanced formability and the fracture mechanism in SPIF. The analytical analysis suggested that the deformation takes place not only in the contact zone, but also in the neighbouring wall around the contact zone. In addition, by investigating the hydrostatic stress, it is proved that the fracture tends to occur firstly on the outer side of the wall at the transition area between the contact and non-contact zone. Authors also acknowledged that the proposed model may be only valid for axisymmetric parts or parts with large wall curvature due to the plane strain assumption.

Li et al. [38]developed a FE model with fine solid elements for truncated cone-forming process to investigate the deformation mechanism. This model allows a quantitative study of the deformation behaviour of stretching, bending and shearing during the ISF process. It was shown that the cone-forming process involves a combination of shearing, bending and stretching deformation modes and allow an extensive discussion of the evolution trend and the contribution of each mode.

2.2 Process formability

Over the recent years, different kinds of studies have been conducted with the emphasis on understanding, assessing and improving the formability in the ISF process. Instead of using the forming limit curves (FLCs) for traditional forming processes, the fracture forming limit curves have to be used to characterise the increased formability in ISF. Alternatively, other formability indicators such as maximum forming angle and fracture depth can be also used to evaluate the maximum formability in ISF.

2.2.1 Formability evaluation

Generally, the forming limit curve is defined as a correlation between the major strain ε_1 and minor strain ε_2 in the plane of the sheet metal at the onset of necking failure. These strain values are recorded from a series of experiments under different loading conditions ranging from biaxial tension (stretch forming) to equal tension and compression (deep drawing). The most widely used method of obtaining the FLC is by means of drawing tests of strips with different widths and a hemispherical punch. In the early stage of the development ISF technology, attempts have been made to use the concept of conventional FLCs to evaluate formability limits in SPIF. However, Iseki et al. [39] noticed from the experimental results that ISF allows sheet metal to be stretched much further than that in conventional stamping operations, well beyond the common FLCs. The work performed by Shim and Park [40] also showed that the forming limit diagram in ISF is different from that in conventional forming. It appears to be a straight line with a negative slope in the positive region of the minor strain. Filice et al. [6] argued that this is due to the peculiarity of the loading condition and process mechanics in the ISF process. Plastic deformation ahead of the forming tool is strongly localised and moves progressively along the tool path. As a result, higher strains can be attained in the material before fracture occurs. The experimental tests further revealed that cracks are likely to occur at the corners due to greater deformation than that along part sides. Kim and Park [41] studied the effect of the process parameters (e.g. tool type, tool size, contact friction and sheet anisotropy) on the formability by experiments and FEM analysis. The straight groove tests have been performed and suggested as an appropriate method to evaluate the effects of process parameters on the formability for aluminium sheet. Further tests were performed to investigate the formability compared to stretching and deep drawing processes for forming complex shapes by Park and Kim [42]. Non-traditional FLCs were used to compare the strains in ISF with those obtained by stretching and deep drawing. They concluded that it is possible to form complicated shapes with sharp corners or edges using TPIF because the plane-strain mode of deformation becomes dominant compared to SPIF.

Filice et al. [6] also demonstrated that the failure strain in ISF significantly exceeds that in conventional forming processes by performing pyramids testing, bi-axial stretching and conical shell testing. This was further studied and confirmed by Silva [26], who concluded that the forming limit curve in ISF was determined as a straight line with the negative slope positioned on a positive area of the forming limit

diagram in the principal strain space. As shown in Fig. 9, the fracture forming limit curve (FFL) is well above the conventional limit curve (labelled FLC) used for stamping and deep drawing processes. Silva et al. [25] revisited the failure mechanics in ISF and provided a much deeper insight on the influence of tool radius. This led to the proposal of a new understanding and assessing on formability limits and formation process of fracture in ISF.

From another point of view, Malhotra et al. [29] explored the unique role of material localisation for the enhanced forming limit in SPIF. They combined a fracture model proposed by Xue [30] with finite element analysis to predict material thinning, forming forces and the occurrence of fracture in SPIF. They extensively discussed the effects of five key indicators (i.e. the damage variable, plastic strain, hydrostatic pressure, through-thickness shear and fracture strain) on the occurrence of fracture in SPIF. It was concluded that the fracture in SPIF is determined by both local bending and shear. In the view of the local nature of the deformation in SPIF, they further proposed a so-called noodle theory, as illustrated in Fig. 10, to explain the increased formability in SPIF. It was shown that the inherently local nature of deformation in SPIF allows the generation of a larger region of unstable deformation. However, this unstable region will not be deformed to fracture as the tool has passed to other regions following the tool path before fracture. These unstable regions play a role of sharing some of the deformation in the subsequent passes of the tool and argued as the primary reason for the enhanced formability.

Although strain analysis is helpful in understanding the mechanics of ISF, the FLCs still have limitations to examine material formability since the process integrating effects of through-thickness shear, bending and cyclic loading [43].

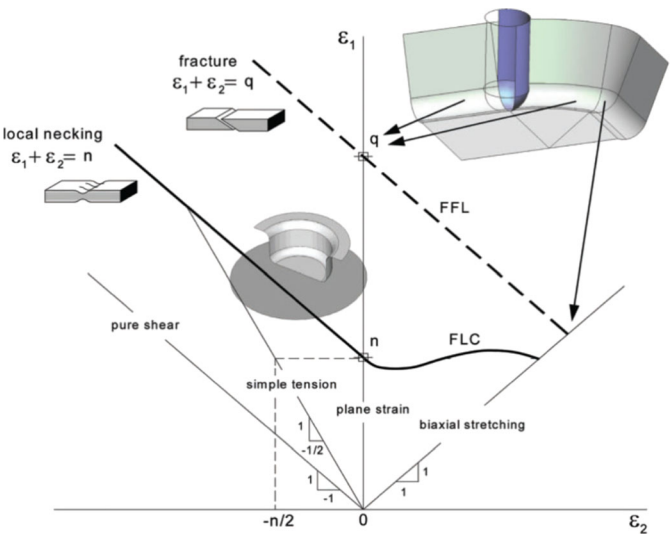

Fig. 9 Schematic representation of the forming limits of SPIF (labelled *FFL*) against that of conventional stamping and deep-drawing processes (labelled *FLC*) in the principal strain space (ε_1 , ε_2) [26]

The maximum formable wall angle has been recognized as an indicator for formability by many researchers. Ham and Jeswiet [44] carried out a design of experiments to study the effect of process parameters (material thickness, step size and tool size) on the forming angle. Also, Capece Minutolo et al. [45] successfully evaluated the formability of both truncated pyramids and cones by using the maximum forming wall angle. A set of experiments was designed by Bhattacharya et al. [46] using the Box-Behnken method to study the effect of the process variables on maximum formable angle. It was found that formable angle first increases and then decreases with step down size varying from 0.2 to 0.8 mm. Hussain and Gao [47] firstly proposed an effective method to obtain the maximum wall angle through a single test by varying wall angle in conical frustum tests. Additionally, truncated cones with a continuously varying wall angle have been used by Fratini et al. [48] and Hussain et al. [49] to reduce the number of experiments required to determine the forming limit.

The fracture depth can also be regarded as another useful geometric formability indictor in ISF. This is more feasible due to the fact that a part with forming angles higher than the critical one can still be formed for a small height. For example, according to Li. et al. [50], the fracture depth for forming a 70° conical cone was 23 mm. The fracture depth was used by Fiorentino et al. [51, 52] to evaluate the effect of tool path on the process formability in TPIF with steel sheets. Ambrogio et al. [53] also evaluated the formability of lightweight alloys by fracture depth in a hot incremental sheet-forming process.

2.2.2 Effects of process parameters on formability

The effects of main process parameters on the ISF formability have been substantially studied in the literature. Jeswiet et al. [1] reviewed that the formability of the process was influenced by four major parameters: (a) thickness of the metal sheet, (b) vertical step-down size, (c) rotational and feed rate speed, and (d) size of the forming tool. The influence of the sheet thickness is commonly explained by the sine law, in which thinning of the material is related to the forming wall angle. The speed of the forming tool is known to influence the formability because it directly affects the frictional conditions at the tool-sheet interface. Smaller radius of the forming tools was claimed to provide better formability due to the concentration of the sheet strains under the forming tool. Larger tool radius tends to distribute the strains over a more extended area and therefore reduces the formability. In terms of step-down size, although Ham and Jeswiet [44] argued that step size does not have significant effect on the formability from their experiments, the general opinion has been that formability decreases with increasing step size (>0.7 mm) [46]. Experimental work from Li et al. [54] showed that the formability was increased with the increase of step-down size from 0.1 mm to 1 mm. The

different observations between this paper and some previous publications are due to two main reasons. First, the investigated range of the step-down size is different. In [50], the step down was set within a small range from 0.1 to 1 mm while larger step-down sizes (>0.7 mm) were used in previous published work [46, 55]. Therefore, there is a possibility that the formability could improve with the increase of the step down at small values (<0.7 mm) and then reduce with the further increase of the value of step down. Second, the size of the forming tool used (30 mm in diameter) is larger than most of the forming tools commonly used. The radius of the tool greatly influences the local bending/shearing of the material ahead of the tool as the sheet has to be deformed to conform to the tool surface. Nevertheless, further detailed investigations of the effects of step down and tool size on the formability are essential to clarify this effect.

Petek et al. [56] analysed the influences of the wall angle, tool rotation, vertical step size, tool diameter and the lubrication on the maximal strains of the formed specimens. The measuring circle grid was printed on the specimens before the forming process and then the deformations of the grid were measured by an optical contactless measurement system. It was observed that with higher wall angles, larger deformations can be obtained for the formed part before cracking. Both tool rotation and lubrication have negligible influence on the maximum strains but it was found the surface quality can be improved by rotating the forming tool with lubrication. Lubrication of titanium and similar metals has been an issue in ISF. Hussain et al. [57] found that using the surface-hardened high speed steel (HSS) tool and the paste of molybdenum disulphide (MoS2) with petroleum jelly is recommended for forming of CP Ti components.

Recently, Xu et al. [32] further explored the mechanism and formability variations induced by tool rotation in the SPIF process. The maximum formable wall angle and fracture depth were regarded as the indictor for assessing the formability. First, the effect of tool rotation was investigated through a series of experiments by varying rotation speed from 0 to 7000 rpm. Four stages were identified depending on different roles of friction and heat during of the forming process. At low tool rotation speed range (0–1000 rpm), friction was found as the dominant factor for formability variation. Nevertheless, the thermal effect on material properties became the most influential factor for formability improvement at high tool rotation speed range (2000–7000 rpm). It was pointed out that the heat generated by friction is enough to activate the dynamic recrystallisation of the material when the speed is above 3000 rpm. Moreover, a laser surface textured (LST) forming tool was introduced to investigate its influence on material formability. It is expected that the LST is able to reduce friction at the tool-workpiece interface, thereby reduce the heat generation especially for a high rotation speed. Accordingly, the formability is reduced due to the decreased thermal effect.

Previous literature shows that effects of process parameters on formability are interactive and vary from material to material. As an example, feed is significant for titanium and steel but not very significant for aluminium. Al-Ghamdi and Hussian [58] compared the formability of roll-bonded steel-Cu composite sheet metal between ISF and stamping processes and found that the formability enhance rate for composite sheet in ISF is 923% which is much greater than that for monolithic sheets (182–268%) [49].

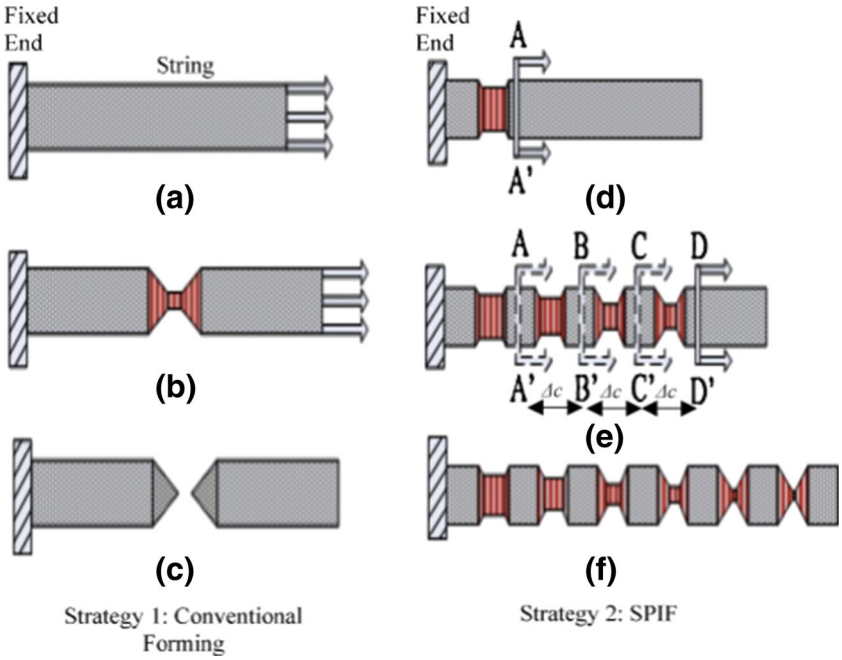

Fig. 10 **a** Stretching the string at the free end. **b** Material necking at a single location. **c** Fracture at location of material necking. **d** Stretching the string at section *A*. **e** Apply loads at a distance after necking locations. **f** Elongation to a greater length without fracture [29]

3 Modelling methods for ISF

Modelling of the ISF process is essential for understanding the deformation behaviour, process investigation and optimisation since it is difficult to reveal the detailed deformation history solely through experimental works due to the highly localised characteristic. In this section, recent developments in the modelling of the ISF process are reviewed from two main perspectives: analytical modelling and finite element (FE) modelling.

3.1 Analytical modelling

Analytical study of the process plays a pivotal role in the understanding of fundamentals of the process and the developing of efficient predictive models.

3.1.1 The sine law

The sine law is a simple geometrical model for sheet thinning in ISF to predict sheet thickness after deformation. This model was previously used in shear spinning by Avitzur and Yang [59], based on the assumptions that the deformation in shear spinning is (a) a straight projection of the initial blank onto the mandrel, (b) that the through thickness deformation of the sheet is a pure shear deformation and (c) that volume constancy holds. Figure 11 depicts the relationship between initial (t_0) and deformed (t_1) sheet thickness for a given wall angle α.

The following equation can be derived based on the assumptions above:

$$t_1 = t_0 \sin\left(90^\circ - \alpha\right) = t_0 \cos\alpha. \tag{4}$$

For the non-flat areas, an alternative '3D version' of sine law is more convenient [60]. The surface of the product can be meshed using triangular and quadrilateral elements thereby the thickness can be calculated as a function of the area ratio of the undeformed and deformed elements. This can be expressed as

$$t_1 = t_0 \frac{A_0}{A}. \tag{5}$$

Kim and Yang [20] used the above equation to compute the sheet thinning for two simple shapes, an ellipsoid and a clover cup. A good conformance between calculations and measurements was achieved for areas that have a shallow curvature. Good qualitative agreement with experimental results were also obtained by Iseki [61]. However, considerable deviations occurred for areas with bending or necking deformation as reported by Young and Jeswiet [62]. To conclude, the sine law provides approximations of sheet thinning for ISF at negligible computational cost, but as a plane strain model it can be applied only when plane strain deformation prevails.

3.1.2 Geometrical model based on intermediate shapes

Bambach [60] devised a simplified geometrical model to allow for a more accurate calculation of the sheet thickness after forming, to predict strain states after forming and to visualise the forming kinematics. This model is based on the assumption that material points between intermediate stages proceed along the normal direction of the current surface. A cone with some intermediate stages is shown in Fig. 12.

In 2D axisymmetric cases, a first-order ordinary differential equation system was developed and expressed by the tool radius R_T and the wall angle α to obtain insight into the material flow. An implementation of the model based on triangular meshes was presented in 3D cases. A new version of the algorithm was developed to calculate the triangulated intermediate stages. The model was used to simulate a pyramidal benchmark part to compare the results with experimental data and the sine law (see Fig. 13). It was concluded that the geometrical model predicts smoother transitions between areas of different inclination, which is more realistic than the abrupt changes predicted by the sine law.

However, there are limitations to this model. Material character and friction are not included while bending effects are neglected. As a result, a promising approach to improving this model would be to couple it with a membrane analysis as proposed in [22, 23].

3.1.3 Energy-based modelling

Raithatha et al. [63] developed a model that is based on the numerical minimisation of internal work within the material. In this method, the minimisation of plastic work was formulated as a second-order cone programming (SOCP) optimisation problem and was solved efficiently using primal dual interior point SOCP algorithms. The results showed that the computing time is 5–9 min for a straight line indentation on a sheet with dimensions of 0.1 m × 0.1 m. However, the reduced computing time was achieved at a loss of model accuracy which results in some fluctuation at the roof of the groove. In this model, only the stretching component of work within the sheet was modelled and was found to be numerically unstable except for very small time increments. To further regulate the simulation, this model was further developed and presented in [64], where the model was improved by incorporating bending work and using finite element discretisation. The modified model showed good geometric agreement compared with measurements from a real product. Nevertheless, the model is not suitable for design and feedback control because the running time was at the same level with the FE model for several hours.

3.2 Finite element modelling

The changing contact condition inherent to ISF makes it a highly computational time-consuming process to model with both implicit and explicit FE codes [33, 65]. In order to use FE to understand and explain the temporal deformation mechanics, dedicated strategies for incremental sheet-forming simulations need to be developed.

Henrard et al. [66, 67] modelled a 40° pie shape to represent the full cone-forming process. The partial models were compared to the full models in [68], showing that although the side wall was reproduced well with partial models, significant deviations were observed in the undeformed zone of the sheet. Moreover, Eyckens [69] have developed a model with fine (sub-millimetre) meshing only at the small plastic zone with continuum elements to avoid excessive computation time. In this way, the through-thickness shear was predicted close to experimental results. However, Jackson and Allwood [24] recommended that FE modelling that considers the full tool path should be employed according to the experimental observation that the strains sustained by any given element of material in ISF are not the same at any position.

Lasunon and Knight [70] confirmed that FE modelling can be used to investigate various aspects of ISF processes by validation with experimental testing with truncated pyramids. Yamashita et al. [71] investigated the applicability of the dynamic explicit finite element code DYNA3D for the simulation of an incremental sheet-forming process of quadrangular pyramids. The effect of the tool path on deformation behaviour was simulated which showed that the starting position of the forming should be at one of the corners. In this case, the step-pattern deformation at the final product can be considerably mitigated compared with other starting positions. Ma and Mo [72] found that FE modelling based on solid elements is more suitable than shell elements to simulate the SPIF in terms of deformation prediction. Dejardin et al. [73] conducted a numerical analysis using LS-DYNA software to predict the springback effect through the cut rings method. It was found that the finite element model with shell elements is not suitable for all tool path strategies to capture the transverse shear behaviour of the sheet. Further work with FE models using elements able to properly reveal the shear components was suggested.

Regarding the use of material models, Flores et al. [68] showed that the use of an anisotropic yield criterion is not a key factor in terms of the geometric prediction of a cone wall. Also, Ambrogio et al. [74] presented that the sheet material orientation has no substantial effect on the predicted straining history with an anisotropic material constitutive law. In [33], the effect of anisotropy in the FE model constitutive law onto the complete strain history was further explored. It was also concluded that the choice of the anisotropic Hill yield locus has no significant improvement compared to von Mises.

Some other researchers [75, 76] have been focusing on contact optimisation in FE simulation. The penalty method has been usually used to deal with contact problems by checking the contact at nodal or integration points. This implies that the force history becomes dependent on the relative position of the tool and also the points where contact is evaluated when the element size is large. Henrard et al. [67] presented a new approach that accounts for contact anywhere inside a small number of elements without using a penalty method. This method is based on a dynamic explicit scheme which has the advantage that no system of equations needs to be solved. The finite element code used was Lagamine that has been developed at the University of Liege for 20 years. The contact algorithm was proven to be more accurate but the computation time was minimal by using a larger element size.

Malhotra et al. [29] developed a finite element model in which a damage plasticity model proposed by Xue [30] was implemented. This model combined the effects of hydrostatic pressure, plastic strain and shear on fracture and it was embedded into a FEA model using a user subroutine in LS-DYNA. The predicted results from the calibrated FE model showed a good agreement with experimental results in terms of vertical forming force, the maximum thinning and the fracture depth. Recently, Smith et al. [34] analysed the deformation mechanics

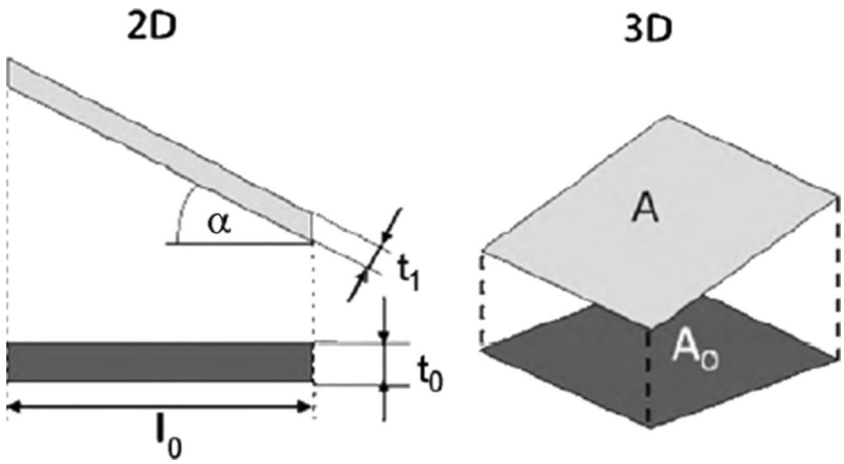

Fig. 11 Illustration of the sine law in 2D and 3D [60]

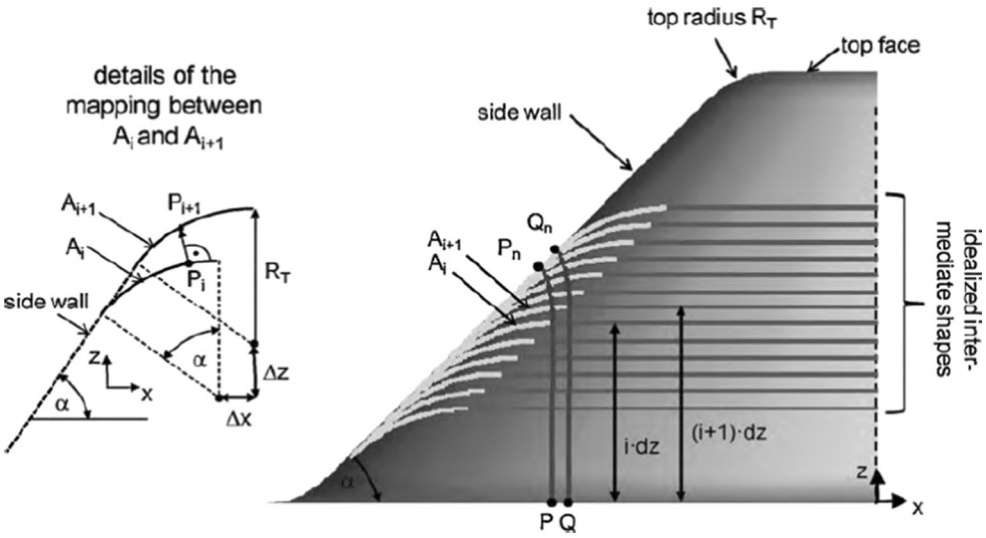

Fig. 12 A cone with some intermediate stages and the trajectories of two adjacent points *P* and *Q* [60]

of both single-point and accumulative double-sided incremental forming (ADSIF) process by FE simulation using LS-DYNA explicit software. Solid elements were used in the described FE model to show the evolution history of plastic strain, hydrostatic pressure, and shear strains parallel and perpendicular to tool motion. It was concluded that the ADSIF could present greater plastic strains, through-thickness-shear strains and greater hydrostatic pressure than in SPIF and suggested this might be the reasons for the increased formability in ADSIF. An efficient model was recently developed by this group for ADSIF by proper setting of tool speed, mesh size, element type and amount of mass scaling [77].

Unlike the majority of numerical simulations which use the flow rule method to determine the elasto-plastic state of the workpiece. Robert et al. [78, 79] proposed a simplified elasto-plastic scheme based on the incremental deformation theory of plasticity. A significant reduction of calculating time (70%) was achieved for the stretching test of a spherical cup using the new algorithm. However, although it provided a better results for geometry prediction, only a small (4%) improvement was obtained for simulating incremental forming process where the localisation of the contact between the tool and the sheet (high contact non-linearity) are dominant. Adaptive remeshing technique using solid-shell elements was implemented by [80] to reduce the computing time. Similarly, an adaptive remeshing strategy combined with subcycling was developed and applied to simulating ISF process [81]. It is shown that simulating time can be reduced up to 80% with acceptable loss of accuracy.

A summary of the characters of the above main predictive models proposed for the ISF are listed in Table 2. Several analytical models are available for efficient estimation of thickness prediction and/or strain calculation, but large deviations could be expected with experimental results. Despite the advances in the finite element analysis for modelling of metal forming processes, existing FE models for the ISF are still computationally inefficient so reducing computational time is still a challenge. Over the past few years, different kinds of customised numerical models have been proposed in the effort to improve computational efficiency with reasonable accuracy.

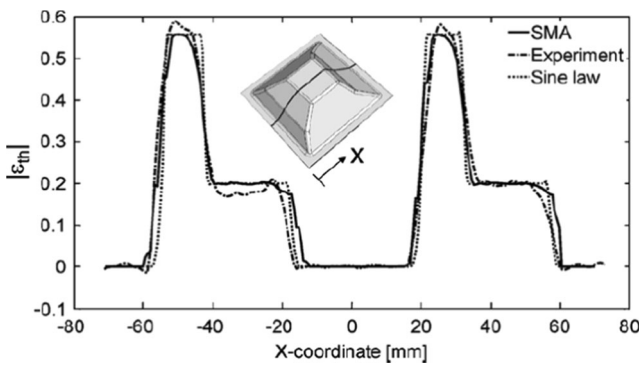

Fig. 13 Comparison of major strains predicted by the simplified modelling approach [60]

4 Forming forces in ISF

Investigation of forming forces in ISF is of great importance since it provides understanding of the deformation mechanics, monitoring of the forming process, failure prediction, and future means of on-line control and optimisation. This section provides a review of studies on the contact conditions and the effects of the process parameters on forming forces in ISF, followed by the current status on forming force prediction and its potential role in the improvement of ISF technology.

4.1 Effects of process parameters on forming forces

Forming forces during ISF have been experimentally studied intensively. Minutolo et al. [82] worked on force analysis in a

groove test and found that using a tool with a bigger diameter, higher drawing depth, higher forming forces and a different typology of failure can be observed. In 2004, Szekeres [83] designed and successfully manufactured a complete system for measuring, recording and processing the forming forces acting on the sheet metal during ISF. They used a spindle mounted cantilever beam with strain gauge Wheatstone bridges, with each bridge designed to measure one of three orthogonal forces: two bending directions, and one axial direction. Szekeres et al. [84] further identified the detailed features of the forming force in ISF using the developed tool with force sensors mounted. It was found that failure in the cone-forming process can be intuitionally predicted by a drop in the total force but this is not readily apparent for the pyramid-forming process. This force measurement system has also been successfully used for measuring the forces in a TPIF configuration [85].

Duflou et al. [86] presented another experimental platform which is capable of measuring three components of forces during the ISF process to investigate the influence of the three process parameters on forming forces: the vertical step size, the tool diameter and the wall angle. More detailed results are described in [87] which further considered the effects of the sheet thickness and lubrication. As shown in Fig. 14, experiments were carried out using a 3-axis CNC vertical milling machine and a table type force sensor was mounted between the fixture and the milling machine work platform. The force sensor was a Kistler 9265 force dynamometer and connected to a Kistler 5017A 8-channel charge amplifier for good data recording performance. A series of experiments were performed with Al 3003-O sheet material by varying step size, wall angle, tool diameter and sheet thickness. Conclusions can be drawn from the experimental measurements as follows:

- As step size increases from 0.25 to 1.0 mm, it is apparent that both the magnitude of the peak and average force after the peak rises and fits well as a linear function.
- Similar to the effect of step size, measured forces are also linearly proportional to the tool diameter in the range of 10 to 30 mm.
- In terms of the wall angle, the magnitude of the force needed gradually increases with the increase of wall angle. Significant peaks can be observed for a part with 60° wall angle which is suggested as a possible indication of material fracture.
- The sheet thickness is a dominant factor determining the magnitude of the resultant force. The required force was increased from 380 to 1460 N by varying the sheet thickness from 0.85 to 2.0 mm.

Petek et al. [56] presented experimental equipment for forming force measurement in SPIF. Forming forces were measured using a dynamometer Kistler 9239 and amplified by Kistler 5001 for analysis. It was found that when increasing wall angles, the forming force is progressively enlarged. Both tool rotation and lubrication have no considerable influences on forming forces but have significant influence on the quality of the surface. The increase of the tool diameter and vertical step size resulted in larger forces. The authors [88] also proposed an autonomous on-line system for fracture identification and localisation by analysing the reaction force with a skewness function.

Another research group has also conducted intensive experimental work on forming force measurements. Filice et al. [89] worked on force analysis and classified

Table 2 Comparison between different predictive models in ISF

Model/paper	Theory/methodology	Advantages	Limits
The sine law [59]	Straight projection Volume constancy	Negligible computational cost	Does not hold for a non-plane deformation
Bambach [60]	The deformation between intermediate shapes proceeds along the surface normal direction	Membrane strain and sheet thickness are predicted	Does not take into account the material behaviour or friction between sheet and tool
Silva [22]	Membrane analysis	Provides a closed-form analytical model for SPIF	Neglecting bending effects and based on SPIF configuration
Henrard [67]	Contact modelling based on a dynamic explicit time integration scheme	It uses actual location instead of fixed positions (e.g. integration or nodal points); larger elements can be used	Simulations were not as accurate as those performed with an implicit strategy; no significant reduction in overall computation time as expected
Robert [79]	Incremental deformation theory	Save 70% computing time for deep drawing with accurate results	Time benefit is small (4%) for ISF
Raithatha [64]	Second-order cone programming based on minimisation of internal work. The rigid perfectly plastic deformation is used	It presents an alternative shell model for incremental deformation	Longer running time(8 h) compared with LS-DYNA (5.5 h)

the trends of tangential force into three types: steady-state force trends, polynomial force trends and monotonically decreasing force trends. In addition, a statistical analysis was performed based on a proper design of experiments (DOE) considering four process parameters at three levels. In particular, the force gradient after the peak was defined and its relation with four process parameters was investigated. It was stated that the force gradient after the peak is highly affected by sheet thickness and wall angle and their interaction, followed by the effects of step size and tool diameter. Ambrogio et al. [90] concluded that the force gradient after the peak can be effectively considered as a critical indicator to detect and prevent workpiece fracture. Moreover, the critical gradient value does not seem to depend on previous process history based on a wide experimental activity. Therefore, forming force is a potential indicator for forming limits identification. Based on the understanding of the effects of each process parameter, a strategy of monitoring and control of force was developed to avoid failure of the produced parts.

4.2 Prediction of forming forces

As suggested previously, forming forces in ISF provide further insights into the deformation mechanics, monitoring of the forming process, failure prediction and a means of on-line control and optimisation; therefore, the efficient prediction of forming force would greatly facilitate the advancement of ISF technology.

Although finite element modelling technology has been widely used in the ISF process for geometric prediction, the accurate prediction of forming forces within a reasonable computational time is still a challenge. Flores et al. [68] recommended that the model identification of both yield locus shape and the hardening behaviour is essential for reasonable force prediction from FE models. The mixed hardening model presented better prediction of forces compared to Von Mises or Hill constitutive laws with isotropic hardening. Bouffioux et al. [91] also found that the conventional methods used to identify material data by a combination of tensile and cyclic shear tests was not adapted to the SPIF process on aluminium alloy AA3103. The 'line test' performed on an ISF machine was proposed to adjust the material parameters and was shown to have better prediction in terms of forming forces. Cerro et al. [92] simulated the SPIF process of a pyramid with a 75° wall angle using shell elements and obtained a 5% difference between the maximum values of the measured and calculated vertical forces. Henrard et al. [66] comprehensively compared the prediction accuracy of FE models in terms of forming forces with two different codes (Abaqus and Lagamine) and several constitutive laws (an elastic-plastic law coupled with various hardening models). It was concluded that three factors: the choice of element type, the constitutive law and the identification procedure for material parameters have considerable influence on force prediction. An inverse material identification procedure with line test was a key factor in accurate force modelling in the ISF process. In addition, it was confirmed that the description of the material behaviour through the thickness is also crucial so brick elements were recommended in FE models. In this study, the highest accuracy was attained in the case where brick elements with a fine mesh were used with a material model that combined the isotropic yield locus of von Mises with the mixed isotropic–kinematic hardening model of Voce–Ziegler. However, due to the localised contact

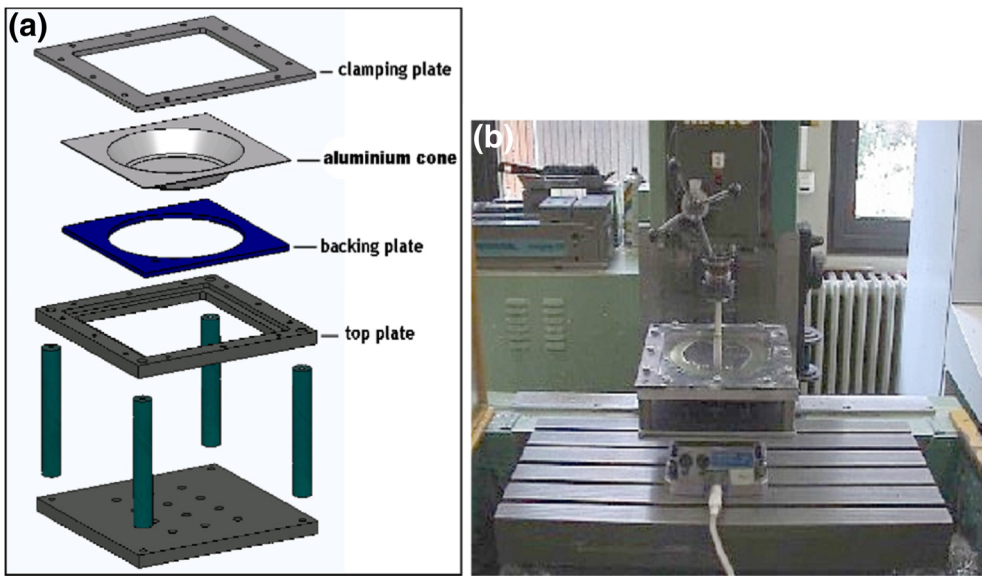

Fig. 14 The experiment setup: **a** exploded view of forming fixture with formed cone; **b** the forming fixture with the force sensor mounted on the machine table [87]

condition and long tool path in ISF, force prediction with FE models is significantly time-consuming. Smith et al. [34] reported a simulation time of 24 days for a single point incremental forming process for a truncated cone shape.

Currently, very limited analytical models are available for the efficient prediction of forming forces in ISF although some researchers have attempted to bridge the existing research gap. To overcome the above computational challenges of the FE approach, Iseki [61] derived the forming force for the incremental forming of a pyramid using a simple approximated deformation analysis based on a plane-strain deformation. The proposed numerical model allowed a systematic investigation of the effects of process parameters on the forming force and thickness distribution. However it was only a rough estimation and has not been validated by wider experimental results. Raithatha and Duncan [64] developed a model based on numerical minimisation of internal work within the material. In this method, the minimisation of plastic work was formulated as a second-order cone programming (SOCP) optimisation problem. By sacrificing the accuracy, a process of straight line indentation on a sheet with dimensions of 0.1 m × 0.1 m was obtained in 9 min. However, the reduced computing time was achieved at a loss of model accuracy which results in considerable fluctuation at the roof of the groove. Moreover, only the stretching component of work within the sheet was modelled and the model was found to be numerically unstable for a full-scale forming process.

Aerens et al. [93] studied the forces in incremental forming of truncated cones with different materials using experimental and statistical analyses. Regression formulae were proposed to predict the triple forming forces including axial, radial, and tangential components at their steady state from input variables including wall angle, initial thickness, tool diameter and step down. In addition, a general model has been presented which can estimate the vertical force component for any material by knowing tensile strength only. Good prediction precision of forming forces was obtained in all tested materials with different working conditions of the cone-forming process. Nevertheless, the proposed model pays little attention to the physical mechanics of the forming process so the contribution to the further optimisation of the process is limited.

More recently, Mirnia an Dariani [28] conducted an upper-bound analysis for a truncated cone-forming process to predict the tangential force using an assumed deformation zone. In this analysis, an assumed deformation zone represented by a series of flow lines was defined and used to calculate the dissipated power. In particular, shear deformation mode is assumed to be the dominant mechanism in the cone-forming process. Later, Li et al. [19, 50] developed a combined model in which the weight of different deformation modes is determined by values of the wall angle and step-down size to reflect the actual deformation mechanism. This is the first reported efficient force prediction model considering all the main deformation modes in ISF. The influences of four process parameters including step size, sheet thickness, tool diameter and wall angle on the tangential force and the equivalent strain were investigated. It was reported that the forces were in good agreement with experimental results reported by Aerens et al. [93]. However, large errors can be expected for severe deformation conditions (e.g. $\Delta z > 0.5$ mm) and may possibly due to the limit of the pure shearing assumption of plastic deformation. Also, the model needs to be further verified with various geometric shapes.

5 Forming quality of ISF

5.1 Geometric accuracy

Presently, the geometric accuracy for ISF products is still one of the biggest challenges for both academic researchers and industrial users. Allwood et al. [94] reported that the specification of geometric accuracy from industrial users for metal sheet components are typically within ±0.2 mm over the whole surface of a part, while the geometric error for ISF currently only achieved around ±3 mm. They [95] also summarised the geometric accuracy in the ISF process into three definitions, i.e. (a) clamped accuracy, (b) unclamped accuracy and (c) final accuracy. Research has been mainly aimed at improving the clamped accuracy. Micari et al. [96] further categorised shape accuracy in ISF into three different typologies as shown in Fig. 15: (a) sheet bending close to the major base of the part where plastic deformation starts, (b) sheet springback after lifting the forming tool and (c) pillow effect on the minor base of the product. The effects of process parameters on geometric error and possible strategies to improve the accuracy are reviewed in this section.

5.1.1 Effects of process parameters on geometric accuracy

The effects of process parameters on geometric accuracy have been investigated through both numerical modelling and experimental methodology. Essa and Hartley [97] investigated the effects of adding a backing plate, a supporting kinematic tool and modifying the final stage of the tool path on the improvement of the geometrical accuracy through a FE model. It was found that the sheet bending near the initial tool contact location can be minimised by the backing plate; the springback can be reduced by the kinematic tool; and the pillow effect can be eliminated by extending the tool path across the base of the sheet.

Guzmán et al. [98] simulated a two-slope SPIF pyramid with two different depths using the FEM to investigate the geometric deviation at the slope transition zone. It was concluded that elastic strains due to structural elastic bending were the main causes of the shape deviations. The localised springback has only minor contribution because no plastic deformation is observed in the angle transition zone. It was recommended that tool path designs could be designed to consider these elastic strains in order to achieve the intended geometry.

Ambrogio et al. [99] statistically analysed the effects of process parameters of tool diameter, step down, wall angle, final product depth and the sheet thickness on geometric accuracy of the formed truncated cone. It was suggested that the geometric error measured at the corner was largely influenced by sheet thickness and total part depth. On the other hand, the pillow effect at the middle of the base was strongly affected by the tool diameter and product height.

Ham [100] performed a Box-Behnken design with 46 experimental tests that considers five factors varied at three levels to study their effects on dimensional accuracy. The five investigated factors include material type, sheet thickness, tool size, step-down size and formed shape. The formed shapes were scanned using a ShapeGrabber® laser scanning system and processed by IMAlign™ software. It was observed that the geometric deviation at the bottom of the formed shape is small compared with the remaining area and the overall geometric error for most of the parts is within 1 mm after a user defined scale. However, only qualitative comparisons were provided based on several contour plots of geometric deviations in this study and further qualitative investigation is required.

Moreover, the geometric accuracy defined as vertical deviations between designed and formed parts has been empirically predicted by quadratic equations giving the influence of the most influential forming parameters [101]. It was concluded that the geometric quality is largely determined by the quadratic effect of wall angle, the linear effect of sheet thickness and the interaction effect of thickness and step down. Decreasing the step-down size was found to be helpful for improving the geometric accuracy.

5.1.2 Strategies to improve geometric accuracy

Current responses to the problem of accuracy in incremental sheet forming can be summarised as the following three main approaches:

(a) Additional support

A variety of additional support configurations have been adopted since ISFs inception. Initially, Iseki et al. [39] utilised a stiff backing plate under the undeformed sheet to prevent unwanted bending, and this remains an effective strategy to maintain reasonable geometric accuracy. The use of both male and female dies has shown benefits to capture the detailed features of the product but with the loss of flexibility of the ISF process. To this end, the use of partial die or a static post was recommended by Matsubara [102]. Interestingly, instead of adding extra supporting, Allwood et al. [95] demonstrated an approach to reduce geometric error by introducing partial cut-outs to locally weaken the sheet blank. Although this idea theoretically seems promising, the conducted study showed minor impact on the overall geometrical accuracy. Meier et al. [103] and Malhotra et al. [16] used a second tool on the opposite of the sheet acting as a local support and significant improvement of geometric accuracy was obtained.

(b) Tool path compensation

Hirt et al. [104] proposed a tool path correction method based on experiments. After measuring the geometric deviation for the first component formed by the regular ISF process, a correction module was applied to the tool path to achieve a specified geometric tolerance. Attanasio et al. [105] conducted a study on tool path optimisation in TPIF and concluded that a tool path with a small scallop height and variable step depth sizes contributes to better part quality. Malhotra et al. [16]

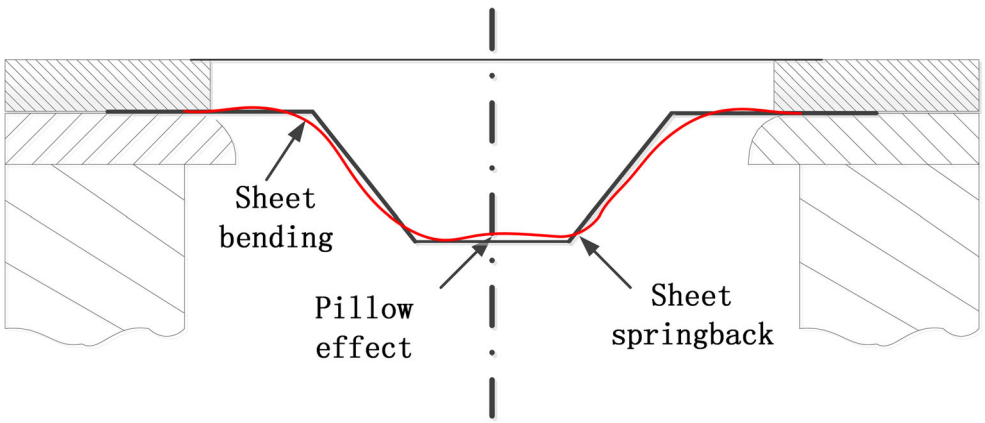

Fig. 15 Geometrical errors during the SPIF process [96]

developed a tool path strategy for DSIF to squeeze the material between the two tools which leads to a faster stabilisation of the deformation into a localised zone around the contact point. A significant improvement in the geometry of the formed component wall was obtained using model predictive control method by Lu et al. [106, 107]. Malhotra et al. [108] also presented an automatic spiral tool path generation algorithm for SPIF, in which the incremental depth is controlled by the geometrical error between the CAD model and formed parts.

Ambrogio et al. [109] performed a robust Taguchi experimental design of ISF with the aim of improving the thickness distribution along with the geometric error by modifying the tool path. In this tool path, an over-slope was applied where the sheet is usually less stretched and a lower angle is imposed where the localised over-thinning usually appears. A FE model was established to simulate and quantify the multi-response optimisation for two considered aims and finally the best process setting for the tool path was provided. Wang and Duncan [110] adopted a closed loop feedback control scheme for generating an optimised tool trajectory. The step depth at each contour for the forming process of a truncated cone was optimised, and a much lower level of geometric error was obtained. However, since current strategies for tool path optimisation are mainly based on experimental measurements rather than deformation theory, further investigation on the applicability of current models to different shapes is essential.

(c) Multi-stage forming

Recent studies have shown that a multi-stage design is also an effective method to improve the geometric accuracy. Bambach et al. [111] showed that multi-stage forming can be applied to improve the accuracy of truncated pyramids manufactured by the SPIF process. It was also identified that local elastic deformation and local springback are the main aspects that limit the improvement of geometric accuracy. The results also suggested that the maximum geometric deviations for the formed parts are reduced with an increasing number of forming stages.

Although various strategies have been proposed to improve product accuracy, the geometric accuracy is still a key concern for ISF developers. Use of a simple backing plate can improve the overall geometric accuracy but is not effective for local deviation improvement. Closed loop feedback control by modifying the tool path during the forming process was recommended as a promising strategy to minimise geometric deviations. Although substantial research work has been conducted on the clamped accuracy, the degradation in unclamped and final accuracy due to residual stresses in the sheet has had very little attention in the literature. Therefore, the effects of process parameters on the unclamped accuracy should be further investigated.

5.2 Forming efficiency and energy consumption

In recent years, environmental and sustainability concerns for metal forming processes have brought considerable attention in the academic world. As for the ISF process, particular attention is focused on the investigation of the forming efficiency and energy consumption under various process parameters and different machine facilities.

5.2.1 Forming efficiency

Due to the long travel of tool movement, forming efficiency (forming time) in ISF is one of the major concerns for practical production. Sarraji et al. [112] studied process forming time in ISF in terms of the effects of four different process parameters (tool diameter, step down size, feed rate and support type). By using Taguchi analysis with design of experiments (DOE) and analysis of variance (ANOVA), the effects of these four process parameters and their combinations were investigated to optimise parameter levels with the aim to minimise forming time. The analysis results showed that the most influential parameter on forming time is step-down size followed by feed rate and then tool diameter.

Ambrogio et al. [113] explored the capability of improving industrial suitability of the ISF process by using very high feed rates to significantly reduce forming time. The effects of high feed rate on formability, surface roughness and geometric accuracy were investigated. It was found that the high feed rates have no considerable effect on formability and surface roughness compared with other process parameters (e.g. step size and tool diameter). In terms of the geometric accuracy, the effect of the tool feed rate and its interaction with the sheet thickness and the wall angle cannot be ignored. However, it was recommended that the tool feed rate can be increased up two orders of magnitude without relevant reduction in the geometrical precision of the component.

5.2.2 Energy consumption

Duflou et al. [114] provided a systematic overview of the energy and resource efficiency improvement methods in the domain of discrete part manufacturing. In terms of the ISF process, three strategies were concluded for reducing the energy usage and improving resource efficiency: (a) redesign of machine tools and selective control, (b) allocating the machine tool at its nominal capacity level and (c) optimising the process parameter settings. Dittrich et al. [12] proposed the concept of exergy analysis (the maximum useful work that can be obtained from a system at a given state in a given

environment) in the ISF process and concluded that the exergy of the sheet material contributed a significant fraction to the total exergy input. Also, compared with conventional forming and hydroforming processes, ISF is advantageous for prototyping and small production runs up to 300 parts from an environmental point of view.

Branker et al. [115] firstly analysed the cost, energy and carbon dioxide emissions in a SPIF process for manufacturing a custom designed aluminium hat. By doubling the feed rate and step-down size, as well as using an eco-benign lubricant, it was found that the cost and energy consumed during the process without labour reduced from $4.48 to $4.10 and 4580 to 1420 kJ, respectively. Additionally, a reduction rate of 31% for the embodied CO_2 was recorded due to the increased feed rate and step-down size. After this, they [116] further investigated sustainability issues in SPIF. In particular, the associated CO_2 emissions were estimated using a life cycle analysis (LCA) approach and costs were calculated using a proposed economic model. The model was firstly implemented in a simple bowl study to find the optimum parameters and then these settings were used to improve the process parameters of a more complex hat shape. It was found that the material of the workpiece dominates the embodied CO_2 emissions in the hat forming process.

Ingarao et al. [117] analysed the energy consumption during both the traditional stamping and the ISF process. The energy consumption was calculated from the recorded forces in all three orthogonal directions multiplied by the corresponding travel distance of the forming tool in that direction. One conclusion has been drawn that the required deformation energy in the ISF process is always higher than that for stamping for all the considered cases, although the ISF process allows a certain material saving. Also, it was suggested that the energy reduction could be obtained through varying the material type, part shape as well as thickness. Recently, Ingarao et al. [118] comprehensively analysed and compared the electric energy consumption of the ISF process by using three different machines: a CNC milling machine, a six-axes robot as well as the dedicated AMINO machine. In terms of the effect of material type of the workpiece, no difference in power demand was observed for CNC milling machine but the six-axes robot was proved to be sensitive to the material type. The AMINO setup is the most efficient machine tool in terms of instantaneous power but requires higher total electric energy due to the lower forming speed compared with the six-axes robot. As far as the process parameters are regarded, increasing the feed rate and step size within the admissible range was recommended as the most effective approach to reduce the energy consumption. In addition, the authors also presented a parametric model to predict the energy consumption for the robot based ISF operations by considering the ultimate tensile strength of the material and the processing time. It should be noted that this model highly depends on the predicting accuracy of the steady vertical force from previous work [93].

Ambrogio et al. [119] compared the power consumption of the SPIF process with two setups: a CNC milling machine and a CNC turning machine. A constant power trend was recorded during the forming step for all the tests due to the fact that loads required to deform the material are much lower than the ones required for the normal operation of machining. It was suggested that the forming time is the dominant factor for energy consumption in the SPIF process. Using the same setup, by reducing the forming time from 144 to 12 s, the energy consumption can be effectively reduced from 838 to 103 kJ. Also, a proper selection and use of machine setup could lead to further saving of energy consumption.

Bagudanch et al. [120] studied the effects of process parameters on the energy consumption. It was concluded that the variation of tool rotation speed is the most significant parameter, followed by the material of the workpiece and step-down size. It was explained that the lower rotation speed greatly reduced the friction between the sheet and the tool and also decreased the processing time since the rotation has to be stopped when the tool descends to the next contour for the machine setup. Unfortunately, the investigated process parameters were only varied at two levels that should be further extended to provide more comprehensive conclusions.

5.3 Surface finish

As a critical product quality constraint, surface roughness is regarded as a weak point in ISF. It is of great importance to identify the impact of forming parameters on the surface roughness and optimise the surface finish at the production stage.

Hagan and Jeswiet [121] analysed the influence of several forming variables, such as step-down size and spindle speed, on surface roughness in ISF process. The authors found that the surface finish can be viewed as a resultant of large-scale waviness created by the tool path and small-scale roughness induced by large surface strains. With the decrease of the step-down size, the morphology of surfaces transforms from waviness to strict roughness without waviness.

Powers et al. [122] investigated the surface morphology through a SPIF case analysis. The effect of sheet rolling mark direction on surface topology in SPIF was first studied. The results showed that surface roughness R_z is greater with rolling marks perpendicular to the forming orientation. Lasunon et al. [123] assessed the effects of three process parameters on the surface roughness in

SPIF by a factorial design. It was concluded that wall angle and step-down size play an important role on the surface roughness, while feed rate has little effect.

Durante et al. [124] described a model for evaluating the roughness in terms of both amplitude and spacing associated with three parameters: the slope angle, the step-down size and the tool radius. The roughness values R_a, R_z, and the mean spacing between profile peaks were evaluated as the output of the models. The prediction showed that a good agreement can be achieved with an error below 10% compared with experimental values. Hamilton et al. [125] investigated the influences of tool feed rates and spindle rotation at high speeds during forming on the non-contact side roughness (i.e. orange peel effect). A model for the orange peel prediction in SPIF was established, which provided some guidelines for the improvement of external surface quality by choosing desirable process parameters during forming. Additionally, lubrication is a critical factor for surface finish in ISF.

Although some research has been performed on the investigation of effects of process parameters on surface roughness and predictive modelling, little research has been focused on the evaluation of overall surface roughness which considers both internal and external surfaces. In addition, the impact of roll mark orientation of metal sheets on surface roughness should be clarified when the surface roughness measurement is carried out along the step down direction.

6 Emerging ISF variants

Recently, to further improve the formability and formed part quality, various assisted forming strategies for ISF has been proposed.

Duflou et al. [126] have developed a laser-assisted incremental forming process (LASPIF) by adding a dynamic heating system. It was concluded from the experimental results that this strategy can provide with a better geometric accuracy, lower forming forces and improved formability. Recently, Duflou et al. [127] further applied this strategy to low angled parts aiming to improve the geometric accuracy by eliminating the bulging deformation. It was found that the proper setting of the local heating results in a significant reduce of the bulge height and the forming forces.

Meier et al. [103, 128] developed the two point incremental forming process with two industrial robots and found that the geometric accuracy could be partially increased by 1 mm compared with the single point configuration. It was also pointed that the improvement of the accuracy is limited by the compliance of the robots. Instead of using robots, Malhotra et al. [16] developed a platform which enables double-sided incremental forming (DSIF). In this configuration, a second tool was used on the opposite side of the sheet, acting as a local support for the forming tool. It was demonstrated that the overall geometry of the components formed with DSIF is much better than that in SPIF by reducing the significant amount of bending at the edges of the component. Therefore, DSIF is a promising ISF strategy regarding the substantial improvement of geometric error of the formed parts.

Water jet incremental sheet metal forming (WJISMF) [129] was firstly reported by Iseki [130]. Then, the forming process of WJISMF was investigated and compared with conventional ISF process by Jurisevic et al. [131]. Li et al. [132] developed a theoretical model for truncated cone forming by WJISMF and found the relationship between forming angle and key process parameters. Recently, Teymoori et al. [133] has performed numerical analysis of WJISMF using coupled Eulerian-Lagrangian approach and found that the sheet thinning happens in the early stage of the process and near the first track of the water jet travelling path.

Electric-assisted incremental sheet forming (E-ISF) [134, 135] were also investigated by researchers which were suggested to be able to improve the formability of the material. The temperature of the sheet can be controlled by adjusting the electric current to fully utilise the formability of sheet material. In addition, E-ISF expanded the application of the incremental sheet-forming process on conventional 'hard-to-form' materials such as titanium alloy [136–138]. However, rough surface of the formed part and sever tool wear are the main challenges of this promising forming strategy.

Electromagnetic incremental forming (EMIF) has been carried out by Cui et al. [139] to form large-scale sheet. In particular, the EMIF process combined with stretch forming has been adopted for manufacturing large-size and thin-walled ellipsoidal parts [140]. During the process, the material sheet was firstly stretched by the pressing plate and then contact with the die due to the coils discharge. It was concluded that the thickness thinning in EMIF is significantly decreased.

Ultrasonic-assisted incremental sheet forming (UISF) is a novel variant of incremental sheet-forming process. Amini et al. [141, 142] designed an UISF system and performed straight groove tests to study the effect of ultrasonic vibrations on the forming process. It was concluded that forming force decreased up to 36% by adding proper ultrasonic vibration to the forming tool. Also, the ultrasonic vibration also improved the formability and reduce the spring back effect, making it a very promising strategy to meet industrial requirements. However, further investigation on the mechanism of these effects is still essential.

7 Summary

A comprehensive review of the current research in ISF technology, including all the major aspects is provided in this paper. Research progress and challenges in each aspect are highlighted based on the relevant studies reported in the literature.

- The extensive previous research has provided valuable insights of the mechanics in ISF and it is recognised that the process involves a complex combination of deformation modes (shear, bending and stretching). However, current findings are limited and sometimes contradictory which may due to various settings of the process parameters and configurations. An agreement has not been reached regarding the role of different deformation modes under various working conditions.
- In terms of the modelling methods in ISF, the geometrical model is good for thickness prediction but material behaviour are not taken in to account. FE models can be used to clarify the forming characteristics, predict forming defects, and improve the forming process, but the models are computationally inefficient, costly and slow due to complicated contact problems involved in the ISF process. Accurate and efficient approaches for modelling the forming process are still lacking.
- The effects of process parameters on forming forces in ISF have been studied mainly through experimental approach. General agreement has been achieved regarding the effects of the most critical factors including step size, tool diameter, sheet thickness and wall angle on forming forces, but the physical explanation behind these phenomena need to be further investigated. The above review of recent studies shows that the prediction of forming forces in ISF has been studied either through time-consuming FE simulations or costly trial experimental tests. There is still a lack of analytical analysis to predict forming forces efficiently.
- It is noticed that despite substantial experimental research into the effects of process parameters on forming forces in ISF, a comprehensive understanding of how process parameters influence the output qualities (e.g. geometric accuracy, surface finish, forming efficiency, etc.) is still essential to clarify the forming process mechanism and thus optimise the process.
- A number of variants of ISF have been proposed by researchers. The forming capacity and part quality have been improved by adopting these strategies. However, research gap still exists between experimental results towards industrial requirements.

Acknowledgements The first author would like to thank the support from National Natural Science Foundation of China (51605258), China Postdoctoral Science Foundation funded project (2016M592180), Key Laboratory of Highefficiency and Clean Mechanical Manufacture at Shandong University, Ministry of Education, and The Fundamental Research Funds of Shandong University.

References

1. Jeswiet J, Micari F, Hirt G, Bramley A, Duflou J, Allwood J (2005) Asymmetric single point incremental forming of sheet metal. CIRP Ann Manuf Technol 54(2):623–649
2. Echrif SBM, Hrairi M (2011) Research and progress in incremental sheet forming processes. Mater Manuf Process 26(11):1404–1414
3. Leszak E (1967) Apparatus and process for incremental dieless forming. USA Patent 3342051A
4. Kitazawa K, WAKABAYASHI A, MURATA K, YAEJIMA K (1996) Metal-flow phenomena in computerized numerically controlled incremental stretch-expanding of aluminum sheets, vol 46. vol 2. Keikinzoku Tokyo, JAPAN
5. Jeswiet J (2001) Incremental single point forming. Transaction of the North American Manufacturing Research INstitution of SME 29:75–79
6. Filice L, Fratini L, Micari F (2002) Analysis of material formability in incremental forming. CIRP Ann Manuf Technol 51(1):199–202
7. Smith J, Malhotra R, Liu WK, Cao J (2013) Deformation mechanics in single-point and accumulative double-sided incremental forming. Int J Adv Manuf Technol 69(5–8):1185–1201
8. Amino M, Mizoguchi M, Terauchi Y, Maki T (2014) Current status of "dieless" Amino's incremental forming. Procedia Engineering 81:54–62
9. Ceretti E, Giardini C, Attanasio A (2004) Experimental and simulative results in sheet incremental forming on CNC machines. J Mater Process Technol 152(2):176–184
10. Ambrogio G, De Napoli L, Filice L, Gagliardi F, Muzzupappa M (2005) Application of incremental forming process for high customised medical product manufacturing. J Mater Process Technol 162–163:156–162
11. Nallagundla V, Lingam R, Cao J (2014) Incremental sheet metal forming processes. In: Nee AYC (ed) Handbook of manufacturing engineering and technology. Springer London, pp 411–452. doi: 10.1007/978-1-4471-4670-4_45
12. Dittrich MA, Gutowski TG, Cao J, Roth JT, Xia ZC, Kiridena V, Ren F, Henning H (2012) Exergy analysis of incremental sheet forming. Prod Eng 6(2):169–177
13. Adams DW (2014) Improvements on single point incremental forming through electrically assisted forming, contact area prediction and tool development. ProQuest, UMI Dissertations Publishing
14. Liu Z, Li Y, Meehan P (2013) Experimental investigation of mechanical properties, formability and force measurement for AA7075-O aluminum alloy sheets formed by incremental forming. Int J Precis Eng Manuf 14(11):1891–1899
15. Vihtonen L, Puzik A, Katajarinne T (2008) Comparing two robot assisted incremental forming methods: incremental forming by pressing and incremental hammering. Int J Mater Form 1(1): 1207–1210
16. Malhotra R, Cao J, Ren F, Kiridena V, Cedric Xia Z, Reddy NV (2011) Improvement of geometric accuracy in incremental forming by using a squeezing toolpath strategy with two forming tools. J Manuf Sci Eng 133(6):61019
17. Allwood J, Houghton N, Jackson K (2005) The design of an incremental sheet forming machine. Adv Mater Res 6:471–478

18. Duflou JR, Callebaut B, Verbert J, De Baerdemaeker H (2008) Improved SPIF performance through dynamic local heating. Int J Mach Tools Manuf 48(5):543–549
19. Li Y, Daniel WJT, Liu Z, Lu H, Meehan PA (2015) Deformation mechanics and efficient force prediction in single point incremental forming. J Mater Process Technol 221:100–111
20. Kim TJ, Yang DY (2000) Improvement of formability for the incremental sheet metal forming process. Int J Mech Sci 42(7): 1271–1286
21. Jeswiet J, Young D (2005) Forming limit diagrams for single-point incremental forming of aluminium sheet. Proc Inst Mech Eng B J Eng Manuf 219(4):359–364
22. Silva MB, Skjoedt M, Martins PAF, Bay N (2008) Revisiting the fundamentals of single point incremental forming by means of membrane analysis. Int J Mach Tools Manuf 48(1):73–83
23. Martins PAF, Bay N, Skjoedt M, Silva MB (2008) Theory of single point incremental forming. CIRP Ann Manuf Technol 57(1):247–252
24. Jackson K, Allwood J (2009) The mechanics of incremental sheet forming. J Mater Process Technol 209(3):1158–1174
25. Silva MB, Nielsen PS, Bay N, Martins PAF (2011) Failure mechanisms in single-point incremental forming of metals. Int J Adv Manuf Technol 56(9):893–903
26. Silva MB, Skjoedt M, Atkins AG, Bay N, Martins PAF (2008) Single-point incremental forming and formability-failure diagrams. J Strain Anal Eng Des 43(1):15–35
27. Allwood J, Shouler D, Tekkaya AE (2007) The increased forming limits of incremental sheet forming processes. Key Eng Mater 344:621–628
28. Mirnia MJ, Dariani BM (2012) Analysis of incremental sheet metal forming using the upper-bound approach. Proceedings of the Institution of Mechanical Engineers, Part B: Journal of Engineering Manufacture
29. Malhotra R, Xue L, Belytschko T, Cao J (2012) Mechanics of fracture in single point incremental forming. J Mater Process Technol 212(7):1573–1590
30. Xue L (2007) Damage accumulation and fracture initiation in uncracked ductile solids subject to triaxial loading. Int J Solids Struct 44(16):5163–5181
31. Lu B, Fang Y, Xu DK, Chen J, Ou H, Moser NH, Cao J (2014) Mechanism investigation of friction-related effects in single point incremental forming using a developed oblique roller-ball tool. Int J Mach Tools Manuf 85:14–29
32. Xu D, Wu W, Malhotra R, Chen J, Lu B, Cao J (2013) Mechanism investigation for the influence of tool rotation and laser surface texturing (LST) on formability in single point incremental forming. Int J Mach Tools Manuf 73:37–46
33. Eyckens P, Belkassem B, Henrard C, Gu J, Sol H, Habraken AM, Duflou JR, Van Bael A, Van Houtte P (2011) Strain evolution in the single point incremental forming process: digital image correlation measurement and finite element prediction. Int J Mater Form 4(1):55–71
34. Smith J, Malhotra R, Liu WK, Cao J (2013) Deformation mechanics in single-point and accumulative double-sided incremental forming. The International Journal of Advanced Manufacturing Technology:1–17
35. Emmens WC, Boogaard AH (2008) Tensile tests with bending: a mechanism for incremental forming. Int J Mater Form 1(1):1155–1158
36. Emmens WC, van den Boogaard AH (2009) An overview of stabilizing deformation mechanisms in incremental sheet forming. J Mater Process Technol 209(8):3688–3695
37. Fang Y, Lu B, Chen J, Xu DK, Ou H (2014) Analytical and experimental investigations on deformation mechanism and fracture behavior in single point incremental forming. J Mater Process Technol 214(8):1503–1515
38. Li Y, Daniel WJT, Meehan PA (2017) Deformation analysis in single-point incremental forming through finite element simulation. Int J Adv Manuf Technol 88(1–4):255–267
39. Iseki H, Kato, K., Sakamoto, S., (1993) Forming limit of flexible and incremental sheet metal bulging with a spherical roller. Proceedings of 4th ICTP, Beijing, China:1635–1640
40. Shim M-S, Park J-J (2001) The formability of aluminum sheet in incremental forming. J Mater Process Technol 113(1):654–658
41. Kim YH, Park JJ (2002) Effect of process parameters on formability in incremental forming of sheet metal. J Mater Process Technol 130–131:42–46
42. Park J-J, Kim Y-H (2003) Fundamental studies on the incremental sheet metal forming technique. J Mater Process Technol 140(1–3): 447–453
43. Allwood JM, Shouler DR (2009) Generalised forming limit diagrams showing increased forming limits with non-planar stress states. Int J Plast 25(7):1207–1230
44. Ham M, Jeswiet J (2006) Single point incremental forming and the forming criteria for AA3003. CIRP Ann Manuf Technol 55(1): 241–244
45. Minutolo FC, Durante M, Formisano A, Langella A (2007) Evaluation of the maximum slope angle of simple geometries carried out by incremental forming process. J Mater Process Technol 194(1–3):145–150
46. Bhattacharya A, Maneesh K, Venkata Reddy N, Cao J (2011) Formability and surface finish studies in single point incremental forming. J Manuf Sci Eng 133(6):61020
47. Hussain G, Gao L (2007) A novel method to test the thinning limits of sheet metals in negative incremental forming. Int J Mach Tools Manuf 47(3–4):419–435
48. Fratini L, Ambrogio G, Di Lorenzo R, Filice L, Micari F (2004) Influence of mechanical properties of the sheet material on formability in single point incremental forming. CIRP Ann Manuf Technol 53(1):207–210
49. Hussain G, Gao L, Hayat N, Ziran X (2009) A new formability indicator in single point incremental forming. J Mater Process Technol 209(9):4237–4242
50. Li Y, Liu Z, Lu H, Daniel WJT, Meehan PA (2014) Experimental study and efficient prediction on forming forces in incremental sheet forming. Adv Mater Res 939:313–321
51. Fiorentino A, Ceretti E, Attanasio A, Mazzoni L, Giardini C (2009) Analysis of forces, accuracy and formability in positive die sheet incremental forming. Int J Mater Form 2(1):805–808
52. Fiorentino A, Attanasio A, Marzi R, Ceretti E, Giardini C (2011) On forces, formability and geometrical error in metal incremental sheet forming. Int J Mater Prod Technol 40(3–4):277–295
53. Ambrogio G, Filice L, Gagliardi F (2012) Formability of lightweight alloys by hot incremental sheet forming. Mater Des 34: 501–508
54. Li Y, Liu Z, Lu H, Daniel WJT, Liu S, Meehan P (2014) Efficient force prediction for incremental sheet forming and experimental validation. Int J Adv Manuf Technol 73(1–4):571–587
55. Jeswiet J, Micari F, Hirt G, Bramley A, Duflou J, Allwood J (2005) Asymmetric single point incremental forming of sheet metal. CIRP Ann Manuf Technol 54(2):88–114
56. Petek A, Kuzman K, Kopač J (2009) Deformations and forces analysis of single point incremental sheet metal forming. Archives of Materials Science and Engineering 35(2):107–116
57. Hussain G, Gao L, Hayat N, Cui Z, Pang YC, Dar NU (2008) Tool and lubrication for negative incremental forming of a commercially pure titanium sheet. J Mater Process Technol 203(1–3):193–201
58. Al-Ghamdi KA, Hussain G (2016) On the comparison of formability of roll-bonded steel-Cu composite sheet metal in incremental forming and stamping processes. Int J Adv Manuf Technol 87(1):267–278

59. Avitzur B, Yang CT (1960) Analysis of power spinning of cones. Journal of Engineering for Industry 82(3):231
60. Bambach M (2010) A geometrical model of the kinematics of incremental sheet forming for the prediction of membrane strains and sheet thickness. J Mater Process Technol 210(12):1562–1573
61. Iseki H (2001) An approximate deformation analysis and FEM analysis for the incremental bulging of sheet metal using a spherical roller. J Mater Process Technol 111:150–154
62. Young D, Jeswiet J (2004) Wall thickness variations in single-point incremental forming. Proceedings of the Institution of Mechanical Engineers, Part B: Journal of Engineering Manufacture 218 (11):1453–1459
63. Raithatha A, Duncan S, Jackson K, Allwood J Second order cone programming in modeling incremental deformation. In, 2007. IEEE, pp 4841–4846
64. Raithatha A, Duncan S (2009) Rigid plastic model of incremental sheet deformation using second-order cone programming. Int J Numer Methods Eng 78(8):955–979
65. Li Y, Liu Z, Daniel WJT, Meehan PA (2014) Simulation and experimental observations of effect of different contact interfaces on the incremental sheet forming process. Mater Manuf Process 29(2):121–128
66. Henrard C, Bouffioux C, Eyckens P, Sol H, Duflou JR, Van Houtte P, Van Bael A, Duchêne L, Habraken AM (2011) Forming forces in single point incremental forming: prediction by finite element simulations, validation and sensitivity. Comput Mech 47(5):573–590
67. Henrard C (2009) Numerical simulations of the single point incremental forming process
68. Flores P, Duchêne L, Bouffioux C, Lelotte T, Henrard C, Pernin N, Van Bael A, He S, Duflou J, Habraken AM (2007) Model identification and FE simulations: effect of different yield loci and hardening laws in sheet forming. Int J Plast 23(3):420–449
69. Eyckens P (2010) Formability in incremental sheet forming: generalization of the Marciniak-Kuczynski model. PhD.Thesis, Katholieke Universiteit Leuven
70. Lasunon O, Knight WA (2007) Comparative investigation of single-point and double-point incremental sheet metal forming processes. Proceedings of the Institution of Mechanical Engineers, Part B: Journal of Engineering Manufacture 221 (12): 1725–1732
71. Yamashita M, Gotoh M, Atsumi S-Y (2008) Numerical simulation of incremental forming of sheet metal. J Mater Process Technol 199(1–3):163–172
72. Ma LW, Mo JH (2008) Three-dimensional finite element method simulation of sheet metal single-point incremental forming and the deformation pattern analysis. Proceedings of the Institution of Mechanical Engineers Part B-Journal of Engineering Manufacture 222 (3):373–380
73. Dejardin S, Thibaud S, Gelin JC, Michel G (2010) Experimental investigations and numerical analysis for improving knowledge of incremental sheet forming process for sheet metal parts. J Mater Process Technol 210(2):363–369
74. Ambrogio G, Filice L, Fratini L, Micari F Process mechanics analysis in single point incremental forming. In: Proceedings of the 8th International Conference on Numerical Methods in Industrial Forming Processes, Columbus, Ohio (USA), 2004. pp 922–927
75. Kim T-J, Yang D-Y (2007) FE-analysis of sheet metal forming processes using continuous contact treatment. Int J Plast 23(3): 544–560
76. Henrard C, Bouffioux C, Godinas A, Habraken A Development of a contact model adapted to incremental forming. In, 2005. The publishing House of the Romanian Academy
77. Moser N, Pritchet D, Ren H, Ehmann KF, Cao J (2016) An efficient and general finite element model for double-sided incremental forming. Journal of Manufacturing Science and Engineering, Transactions of the ASME 138 (9)
78. Robert C, Dal Santo P, Delamézière A, Potiron A, Batoz JL (2008) On some computational aspects for incremental sheet metal forming simulations. Int J Mater Form 1(1):1195–1198
79. Robert C, Delamézière A, Dal Santo P, Batoz JL (2012) Comparison between incremental deformation theory and flow rule to simulate sheet-metal forming processes. J Mater Process Technol 212(5):1123–1131
80. Sena JIV, Lequesne C, Duchene L, Habraken AM, Valente RAF, De Sousa RJA (2016) Single point incremental forming simulation with adaptive remeshing technique using solid-shell elements. Eng Comput 33(5):1388–1421
81. Bambach M (2016) Fast simulation of incremental sheet metal forming by adaptive remeshing and subcycling. Int J Mater Form 9(3):353–360
82. Minutolo FC, Durante M, Formisano A, Langella A Forces analysis in sheet incremental forming and comparison of experimental and simulation results. In: Intelligent production machines and systems-2nd IPROMS virtual internationl conference, 2006. pp 229–234
83. Szekeres AJ (2004) Three axis force measurement for computer numerical control single point incremental forming. MQ92357, Queen's University at Kingston (Canada), Canada
84. Szekeres A, Ham M, Jeswiet J (2007) Force measurement in pyramid shaped parts with a spindle mounted force sensor. Key Eng Mater 344:551–558
85. Jeswiet J, D JR, Szekeres A (2005) Forces in single point and two point incremental forming. Adv Mater Res 6-8:449–456
86. Duflou JR (2005) Force measurements for single point incremental forming: an experimental study. Adv Mater Res 6-8:441–448
87. Duflou J, Tunçkol Y, Szekeres A, Vanherck P (2007) Experimental study on force measurements for single point incremental forming. J Mater Process Technol 189(1):65–72
88. Petek A, Kuzman K, Suhač B (2009) Autonomous on-line system for fracture identification at incremental sheet forming. CIRP Ann Manuf Technol 58(1):283–286
89. Filice L, Ambrogio G, Micari F (2006) On-line control of single point incremental forming operations through punch force monitoring. CIRP Ann Manuf Technol 55(1):245–248
90. Ambrogio G, Filice L, Micari F (2006) A force measuring based strategy for failure prevention in incremental forming. J Mater Process Technol 177(1–3):413–416
91. Bouffioux C, Eyckens P, Henrard C, Aerens R, Van Bael A, Sol H, Duflou JR, Habraken AM (2008) Identification of material parameters to predict single point incremental forming forces. Int J Mater Form 1(1):1147–1150
92. Cerro I, Maidagan E, Arana J, Rivero A, Rodríguez PP (2006) Theoretical and experimental analysis of the dieless incremental sheet forming process. J Mater Process Technol 177(1–3):404–408
93. Aerens R, Eyckens P, Van Bael A, Duflou JR (2010) Force prediction for single point incremental forming deduced from experimental and FEM observations. Int J Adv Manuf Technol 46(9): 969–982
94. Allwood JM, King GPF, Duflou J (2005) A structured search for applications of the incremental sheet-forming process by product segmentation. Proceedings of the Institution of Mechanical Engineers, Part B: Journal of Engineering Manufacture 219 (2): 239–244
95. Allwood JM, Braun D, Music O (2010) The effect of partially cut-out blanks on geometric accuracy in incremental sheet forming. J Mater Process Technol 210(11):1501–1510
96. Micari F, Ambrogio G, Filice L (2007) Shape and dimensional accuracy in single point incremental forming: state of the art and future trends. J Mater Process Technol 191(1–3):390–395

97. Essa K, Hartley P (2011) An assessment of various process strategies for improving precision in single point incremental forming. Int J Mater Form 4(4):401–412
98. Guzmán CF, Gu J, Duflou J, Vanhove H, Flores P, Habraken AM (2012) Study of the geometrical inaccuracy on a SPIF two-slope pyramid by finite element simulations. Int J Solids Struct 49(25): 3594–3604
99. Ambrogio G, Cozza V, Filice L, Micari F (2007) An analytical model for improving precision in single point incremental forming. J Mater Process Technol 191(1–3):92–95
100. Ham MEJ (2007) Single point incremental forming of aluminum sheet metal: The development of maximum forming angle forming limits, measured strains, surface roughness and dimensional accuracy. Ph.D., Queen's University (Canada), Ann Arbor
101. Li Y, Lu H, Daniel WJT, Meehan PA (2015) Investigation and optimization of deformation energy and geometric accuracy in the incremental sheet forming process using response surface methodology. Int J Adv Manuf Technol 79(9–12):2041–2055
102. Matsubara S (1994) Incremental backward bulge forming of a sheet metal with a hemispherical head tool. Journal of the JSTP 35(406):1311–1316
103. Meier H, Magnus C, Smukala V (2011) Impact of superimposed pressure on dieless incremental sheet metal forming with two moving tools. CIRP Ann Manuf Technol 60(1):327–330
104. Hirt G, Ames J, Bambach M, Kopp R (2004) Forming strategies and process modelling for CNC incremental sheet forming. CIRP Ann Manuf Technol 53(1):203–206
105. Attanasio A, Ceretti E, Giardini C, Mazzoni L (2008) Asymmetric two points incremental forming: improving surface quality and geometric accuracy by tool path optimization. J Mater Process Technol 197(1–3):59–67
106. Lu H, Kearney M, Li Y, Liu S, Daniel WJT, Meehan PA (2016) Model predictive control of incremental sheet forming for geometric accuracy improvement. Int J Adv Manuf Technol 82(9–12): 1781–1794
107. Lu H, Kearney M, Liu S, Daniel WJT, Meehan PA (2016) Two-directional toolpath correction in single-point incremental forming using model predictive control. International Journal of Advanced Manufacturing Technology:1–16
108. Malhotra R, Reddy NV, Cao J (2010) Automatic 3D spiral toolpath generation for single point incremental forming. J Manuf Sci Eng 132(6):061003–061003
109. Ambrogio G, Gagliardi F, Filice L (2013) Robust design of incremental sheet forming by Taguchi's method. Procedia CIRP 12: 270–275
110. Wang H, Duncan S Optimization of tool trajectory for incremental sheet forming using closed loop control. In: Automation Science and Engineering (CASE), 2011 I.E. Conference on, 24–27 Aug. 2011 2011. pp 779–784. doi:10.1109/case.2011.6042410
111. Bambach M, Taleb Araghi B, Hirt G (2009) Strategies to improve the geometric accuracy in asymmetric single point incremental forming. Prod Eng 3(2):145–156
112. Sarraji WKH, Hussain J, Ren W-X (2011) Experimental investigations on forming time in negative incremental sheet metal forming process. Mater Manuf Process 27(5):499–506
113. Ambrogio G, Filice L, Gagliardi F (2012) Improving industrial suitability of incremental sheet forming process. Int J Adv Manuf Technol 58(9–12):941–947
114. Duflou JR, Sutherland JW, Dornfeld D, Herrmann C, Jeswiet J, Kara S, Hauschild M, Kellens K (2012) Towards energy and resource efficient manufacturing: a processes and systems approach. CIRP Ann Manuf Technol 61(2):587–609
115. Branker K, Adams D, Jeswiet J (2012) Initial analysis of cost, energy and carbon dioxide emissions in single point incremental forming - producing an aluminium hat. Int J Sustain Eng 5(3):188
116. Branker K, Adams D, Szekeres A, Jeswiet J (2013) Investigation of energy, carbon dioxide emissions and costs in single point incremental forming. In: Nee AYC, Song B, Ong S-K (eds) Re-engineering manufacturing for sustainability. Springer Singapore, pp 291–295. doi:10.1007/978-981-4451-48-2_48
117. Ingarao G, Ambrogio G, Gagliardi F, Di Lorenzo R (2012) A sustainability point of view on sheet metal forming operations: material wasting and energy consumption in incremental forming and stamping processes. J Clean Prod 29–30(0):255–268
118. Ingarao G, Vanhove H, Kellens K, Duflou JR (2014) A comprehensive analysis of electric energy consumption of single point incremental forming processes. J Clean Prod 67(0):173–186
119. Ambrogio G, Ingarao G, Gagliardia F, Di Lorenzo R (2014) Analysis of energy efficiency of different setups able to perform single point incremental forming (SPIF) processes. Procedia CIRP 15(0):111–116
120. Bagudanch I, Garcia-Romeu ML, Ferrer I, Lupiañez J (2013) The effect of process parameters on the energy consumption in single point incremental forming. Procedia Engineering 63(0):346–353
121. Hagan E, Jeswiet J (2004) Analysis of surface roughness for parts formed by computer numerical controlled incremental forming. Proc Inst Mech Eng, B J Eng Manuf 218 (10):1307–1312
122. Powers BM, Ham M, Wilkinson MG (2010) Small data set analysis in surface metrology: an investigation using a single point incremental forming case study. Scanning 32(4):199–211
123. Lasunon OU (2013) Surface roughness in incremental sheet metal forming of AA5052. Adv Mater Res 753-755:203–206
124. Durante M, Formisano A, Langella A (2010) Comparison between analytical and experimental roughness values of components created by incremental forming. J Mater Process Technol 210(14):1934–1941
125. Hamilton KAS (2010) Friction and external surface roughness in single point incremental forming: a study of surface friction, contact area and the 'orange peel' effect
126. Duflou JR, Callebaut B, Verbert J, De Baerdemaeker H (2007) Laser assisted incremental forming: formability and accuracy improvement. CIRP Ann Manuf Technol 56(1):273–276
127. Mohammadi A, Vanhove H, Van Bael A, Duflou JR (2016) Towards accuracy improvement in single point incremental forming of shallow parts formed under laser assisted conditions. Int J Mater Form 9(3):339–351
128. Meier H SV, Dewald O, Zhang J(2007) Two point incremental forming with two moving forming tools. In: SheMet '07 Proceedings of the 12th International Conference on Sheet Metal, Palermo, Sicily, Italy. pp 599–605
129. Sajn V, Jurisevic B, Kosel F (2011) Water jet incremental sheet metal forming: pressure distribution analysis. Int J Interact Des Manuf 5(2):95–102
130. Iseki H (2001) Flexible and incremental bulging of sheet metal using high-speed water jet. JSME International Journal, Series C: Mechanical Systems, Machine Elements and Manufacturing 44 (2):486–493
131. Jurisevic B, Kuzman K, Junkar M (2006) Water jetting technology: an alternative in incremental sheet metal forming. Int J Adv Manuf Technol 31(1):18–23
132. Li J, He K, Wei S, Dang X, Du R (2014) Modeling and experimental validation for truncated cone parts forming based on water jet incremental sheet metal forming. Int J Adv Manuf Technol 75(9):1691–1699
133. Teymoori F, LohMousavi M, Etesam A (2016) Numerical analysis of fluid structure interaction in water jet incremental sheet forming process using coupled Eulerian–Lagrangian approach. Int J Interact Des Manuf 10(2):203–210
134. Fan G, Gao L, Hussain G, Wu Z (2008) Electric hot incremental forming: a novel technique. Int J Mach Tools Manuf 48(15):1688–1692

135. Xu D, Lu B, Cao T, Chen J, Long H, Cao J (2014) A comparative study on process potentials for frictional stir- and electric hot-assisted incremental sheet forming. Procedia Engineering 81(0): 2324–2329
136. Liu R, Lu B, Xu D, Chen J, Chen F, Ou H, Long H (2016) Development of novel tools for electricity-assisted incremental sheet forming of titanium alloy. Int J Adv Manuf Technol 85(5): 1137–1144
137. Honarpisheh M, Abdolhoseini MJ, Amini S (2015) Experimental and numerical investigation of the hot incremental forming of Ti-6Al-4V sheet using electrical current. International Journal of Advanced Manufacturing Technology
138. Magnus CS (2016) Joule heating of the forming zone in incremental sheet metal forming: part 2. The International Journal of Advanced Manufacturing Technology:1–15
139. Cui XH, Mo JH, Li JJ, Zhao J, Zhu Y, Huang L, Li ZW, Zhong K (2014) Electromagnetic incremental forming (EMIF): a novel aluminum alloy sheet and tube forming technology. J Mater Process Technol 214(2):409–427
140. Cui X, Mo J, Li J, Xiao X, Zhou B, Fang J (2016) Large-scale sheet deformation process by electromagnetic incremental forming combined with stretch forming. J Mater Process Technol 237:139–154
141. Vahdati M, Mahdavinejad R, Amini S (2015) Investigation of the ultrasonic vibration effect in incremental sheet metal forming process. Proc Inst Mech Eng B J Eng Manuf
142. Amini S, Hosseinpour Gollo A, Paktinat H (2016) An investigation of conventional and ultrasonic-assisted incremental forming of annealed AA1050 sheet. Int J Adv Manuf Technol r1–10